

Published in final edited form as:

Sci Signal. ; 3(122): ra38. doi:10.1126/scisignal.2000500.

TREM2- and DAP12-Dependent Activation of PI3K Requires DAP10 and Is Inhibited by SHIP1

Qisheng Peng^{1,2}, Shikha Malhotra¹, James A. Torchia³, William G. Kerr⁴, K. Mark Coggeshall⁵, and Mary Beth Humphrey^{1,6,*}

¹ Department of Medicine, University of Oklahoma Health Sciences Center, Oklahoma City, OK 73104, USA

² College of Veterinary Medicine, Jilin University, Changchun 130062, China

³ Department of Medicine, University of California San Francisco, San Francisco, CA 94121, USA

⁴ Department of Microbiology & Immunology and Pediatrics, State University of New York Upstate Medical University, Syracuse, NY 13210, USA

⁵ Department of Immunobiology and Cancer Research Program, Oklahoma Medical Research Foundation, Oklahoma City, OK 73104, USA

⁶ Department of Veterans Affairs, Oklahoma City, OK 73104, USA

Abstract

The activation and fusion of macrophages and of osteoclasts require the adaptor molecule DNAX-activating protein of 12 kD (DAP12), which contains immunoreceptor tyrosine-based activation motifs (ITAMs). TREM2 (triggering receptor expressed on myeloid cells-2) is the main DAP12-associated receptor in osteoclasts and, similar to *DAP12* deficiency, loss of *TREM2* in humans leads to Nasu-Hakola disease, which is characterized by bone cysts and dementia. Furthermore, in vitro experiments have shown that deficiency in *DAP12* or *TREM2* leads to impaired osteoclast development and the formation of mononuclear osteoclasts. Here, we demonstrate that the ligation of TREM2 activated phosphatidylinositol 3-kinase (PI3K), extracellular signal-regulated kinase 1 (ERK1) and ERK2, and the guanine nucleotide exchange factor Vav3; induced the mobilization of intracellular calcium (Ca²⁺) and the reorganization of actin; and prevented apoptosis. The signaling adaptor molecule DAP10 played a key role in the TREM2- and DAP12-dependent recruitment of PI3K to the signaling complex. Src homology 2 (SH2) domain-containing inositol phosphatase-1 (SHIP1) inhibited TREM2- and DAP12-induced signaling by binding to DAP12 in an SH2 domain-dependent manner and preventing the recruitment of PI3K to DAP12. These results demonstrate a

*To whom correspondence should be addressed. marybeth-humphrey@ouhsc.edu.

SUPPLEMENTARY MATERIALS: www.sciencesignaling.org/cgi/content/full/3/122/ra38/DC1

Fig. S1. Recruitment of PLC- γ 2 and Grb2 to DAP12 occurs upon ligation of TREM2.

Fig. S2. DAP10 and DAP12 form homodimers and heterodimers in macrophages.

Fig. S3. DAP10 is not required for the expression of TREM2 at the cell surface or for TREM2-induced Ca²⁺ flux.

Fig. S4. Ligation of TREM2 leads to protection from apoptosis by inducing the production of MCL-1.

Fig. S5. Inhibition of PI3K, but not of Src or Syk, increases the amount of SHIP1 recruited to DAP12.

Fig. S6. SHIP1 and DAP10 colocalize with actin in cap-like structures after ligation of TREM2.

Fig. S7. DAP10 is not required for the translocation of SHIP1 to the plasma membrane.

Author contributions: M.B.H. initiated the project; J.A.T. performed initial immunoprecipitation studies, Q.P. and S.M. performed all experiments; M.B.H., Q.P., S.M., W.G.K., and K.M.C. designed experiments and analyzed data; M.B.H. wrote the paper; Q.P., S.M., W.G.K., and K.M.C. edited the paper.

Competing interests: W.G.K. and K.M.C. are advisors to Aquinox Pharmaceuticals. The use of *SHIP1*^{-/-} mice requires a materials transfer agreement (MTA).

previously uncharacterized interaction of SHIP1 with DAP12 that functionally limits TREM2- and DAP12-dependent signaling and identify a mechanism through which SHIP1 regulates key ITAM-containing receptors by directly blocking the binding and activation of PI3K.

INTRODUCTION

Osteoclasts are bone-resorbing cells that differentiate from myeloid precursors. Macrophage colony-stimulating factor (M-CSF) and receptor activator of nuclear factor κ B (NF- κ B) ligand (RANKL) are the master regulators of osteoclast differentiation. We and others have shown that the immunoreceptor tyrosine-based activation motif (ITAM)-containing adaptor proteins DNAX-activating protein of 12 kD (DAP12) and the Fc ϵ RI γ chain are also required for the normal differentiation and function of osteoclasts in vitro and in vivo (1–4). DAP12 is a central participant in multiple signaling pathways that are involved in the development and activation of osteoclasts, including signaling by RANKL and M-CSF and through the activation of integrins (3,5,6). Confirming the key role of DAP12 in the regulation of osteoclasts, *DAP12*-deficient humans with Nasu-Hakola disease and *DAP12*-deficient mice have small, dysfunctional osteoclasts (1–3,7). Furthermore, *DAP12*-deficient mice have mild osteopetrosis with thickened bones and increased bone mineral density that is secondary to osteoclast dysfunction, which indicates that DAP12 is required for homeostatic bone remodeling (8).

DAP12 is a 12-kD homodimer that is found at the plasma membrane where it associates with numerous receptors through paired charged amino acid residues within the transmembrane domains of DAP12 and its associated receptor. In myeloid cells, DAP12 associates with various receptors, including triggering receptor expressed on myeloid cells-2 (TREM2), myeloid DAP12-associating lectin-1 (MDL-1), and signal regulatory protein β 1 (SIRP β), among others (9). DAP12 is activated indirectly through the binding of ligand to its associated receptors or through outside-in signaling from RANKL, M-CSF, or the integrin α _v β ₃ (3,5,6). The nature of DAP12 signaling in these various contexts is not well understood. Unexpectedly, some studies showed that DAP12 is required to down-regulate Toll-like receptor (TLR)-induced production of cytokines and to limit inflammatory responses in vivo (10–13), which suggests that DAP12 may have both inhibitory and activating functions. Thus, a firm understanding of the regulation of DAP12 signaling is critical for further insights into the regulation of innate immune responses and the regulation of macrophages and osteoclasts.

A key DAP12-associated receptor that is required for osteoclastogenesis and for the suppression of TLR-dependent signaling is TREM2, an immunoglobulin-like receptor (7,12–15). Whereas a deficiency in TREM2 in humans leads to the generation of small, dysfunctional osteoclasts (similar to what occurs under *DAP12*-deficient conditions), *TREM2*-deficient mice have accelerated in vitro osteoclastogenesis compared to that of wild-type mice, through an as-yet unknown mechanism (16). We have shown that mouse TREM2 and DAP12 are required for the fusion of preosteoclasts, which is a prerequisite for the generation of large multinuclear osteoclasts (2,14). In vitro, stimulation of TREM2 leads to increases in the numbers of large multinuclear osteoclasts, whereas the introduction of small interfering RNA (siRNA) specific for TREM2 into the preosteoclast monocyte cell line RAW 264.7 results in the impaired multinucleation of osteoclasts derived in vitro by stimulation with RANKL (14). Similar to DAP12, a deficiency in TREM2 leads to the enhanced responsiveness of macrophages and dendritic cells to the stimulation of TLRs (11,12,15,17). This is a unique property of TREM2, because the presence of other DAP12-associated receptors fails to restore normal regulation of TLR signaling (12). Thus, TREM2 and DAP12 may uniquely provide both activating and inhibitory signals depending on their microenvironment.

Although the mechanisms that regulate DAP12 signaling are poorly understood, other ITAM-containing proteins are regulated by coaggregation with receptors that bear an immunoreceptor-tyrosine-based inhibitory motif (ITIM). The ITIM recruits phosphatases to the ITAM signaling complex, including tyrosine Src homology 2 (SH2) domain-containing phosphatase-1 (SHP-1) and SH2 domain-containing inositol phosphatase-1 (SHIP1). The local recruitment of phosphatases inhibits the activating ITAM signals (18). Alternatively, an ITAM may directly recruit a phosphatase in the absence of a coaggregating ITIM. For example, the ITAM-containing adaptor protein Fc ϵ RI γ recruits SHIP1 upon the initiation of phagocytosis, thus leading to restricted phagocytosis (19,20). Similarly, Fc α R1 associates with Fc ϵ RI γ , and the binding of low-affinity ligand to this receptor causes the recruitment of the tyrosine phosphatase SHIP1 to Fc ϵ RI γ , whereas high-affinity binding causes the recruitment of the tyrosine kinase spleen tyrosine kinase (Syk) to Fc ϵ RI γ (21). Alternatively, membrane-bound phosphatases, such as CD45, that are not directly bound to an ITAM-containing protein may inhibit the Src family kinases that are needed to activate ITAM signals (22). SHIP1 is an important regulator of the differentiation and activation of osteoclasts. *SHIP1*-deficient mice are severely osteoporotic and have excessive numbers of osteoclasts, which are highly multinucleated (23). Given that SHIP1 regulates signaling mediated by the ITAM of Fc ϵ RI γ in myeloid cells (19,20), we investigated whether SHIP1 might regulate TREM2- and DAP12-dependent signaling in macrophages and osteoclasts.

RESULTS

SHIP1 inhibits TREM2-dependent osteoclastogenesis

Although inhibitors of TREM2- and DAP12-dependent signaling have not been described, candidate regulators of ITAM-dependent signaling in myeloid cells include the tyrosine phosphatases SHP-1 and SHP-2 and the lipid phosphatase, SHIP1. Because of the unique properties of inhibition and activation of cellular events by TREM2 and DAP12, we hypothesized that the differential recruitment of phosphatases might play a role in the regulation of TREM2 and DAP12 signaling in macrophages and osteoclasts. To identify putative inhibitors of DAP12 signaling in osteoclasts, we performed a functional assay of osteoclast multinucleation in preosteoclasts derived from phosphatase-deficient mice and we looked for enhanced responses to the ligation of TREM2. Preosteoclasts derived from *SHIP1*-deficient or wild-type littermates were generated from bone marrow macrophages (BMMs) and were stimulated with RANKL and M-CSF in the presence of an antibody against TREM2 or an isotype-matched control antibody. As seen previously (2,14), preosteoclasts derived from wild-type BMM precursors stimulated with an antibody against TREM2 produced twice as many osteoclasts compared to those that were untreated or were treated with the control antibody (Fig. 1). Preosteoclasts from *SHIP1*-deficient mice treated with antibody against TREM2 exhibited a fourfold increase in the formation of osteoclasts (Fig. 1) compared to those treated with the control antibody. This effect was independent of the increase in the basal number of osteoclast precursors in the *SHIP1*-deficient cell cultures (Fig. 1). Thus, direct ligation of TREM2 stimulated the multinucleation of osteoclasts, which was substantially increased in the absence of SHIP1. We concluded that SHIP1 regulated TREM2 and DAP12 signaling during the multinucleation of osteoclasts.

SHIP1 is recruited to DAP12 in response to ligation of TREM2

We next explored the molecular mechanism by which SHIP1 could inhibit TREM2 and DAP12 signaling. We first investigated whether SHIP1 was recruited to a DAP12-containing signaling complex. We stimulated the mouse monocyte cell line, J774, by cross-linking TREM2 at the surface with a specific antibody and then subjecting cell lysates to immunoprecipitation with an antibody against phosphorylated DAP12 (pDAP12). Immunoprecipitated proteins were analyzed by Western blotting for the presence of SHIP1 and the analysis revealed the

recruitment of SHIP1 to pDAP12 in an activation-dependent manner, with the strongest association seen 2 min after cross-linking of TREM2 (Fig. 2A). Treatment of J774 cells with sodium orthovanadate, which inhibits the activity of tyrosine phosphatases, induced the increased phosphorylation of DAP12 and enhanced the association of SHIP1 with pDAP12 (Fig. 2A). To verify that the SHIP1-DAP12 association was not unique to an immortalized cell line, we confirmed our results in preosteoclasts that were derived from BMMs from C57BL/6 mice. SHIP1 was constitutively immunoprecipitated with pDAP12 and the amount of SHIP1 that immunoprecipitated with pDAP12 was further increased at 2 min after ligation of TREM2 (Fig. 2B). Thus, ligation of TREM2 in primary macrophages and monocyte cell lines led to the early recruitment of SHIP1 to DAP12.

The recruitment of SHIP1 to DAP12 is specified by the DAP12-associated receptor

To determine whether the recruitment of SHIP1 to DAP12 was a general method for the regulation of DAP12, we investigated two other DAP12-associated receptors that are found in macrophages and osteoclasts, SIRP β and MDL-1. SIRP β is another immunoglobulin-like receptor, whereas MDL-1 is a C-type lectin receptor. J774 cells were stimulated with antibodies against TREM2, SIRP β , or MDL-1 and immunoprecipitations with an antibody against pDAP12 were performed. Similar to TREM2, ligation of MDL-1 induced the recruitment of SHIP1 to pDAP12 (Fig. 2C). Stimulation of SIRP β failed to substantially induce the association of SHIP1 with pDAP12. These results indicate that the regulation of DAP12 signaling by SHIP1 was determined by the specific associating receptor.

SHIP1 inhibits the activation of TREM2 and DAP12 signaling in preosteoclasts

We next investigated the signaling pathways downstream of TREM2 and DAP12 that were regulated by SHIP1 by performing experiments in which we cross-linked TREM2 in BMMs derived from wild-type and *SHIP1*-deficient mice. Cross-linking of TREM2 induced the activation or recruitment of the components of multiple cellular pathways to a DAP12 signaling complex. In wild-type cells examined 2 min after the ligation of TREM2, these pathways included the phosphorylation of the survival protein Akt and the activation of ERK1 and ERK2, which is needed for transcriptional regulation (Fig. 2D). Proteins that are critical for the normal control of the cytoskeleton in osteoclasts, including Syk and Vav3, were also phosphorylated at 2 and 5 min after ligation of TREM2 (Fig. 2D). In the absence of SHIP1, ligation of TREM2 increased the extent of phosphorylation of Akt, ERK, Vav3, and Syk compared to that in wild-type cells (Fig. 2D).

Because DAP12 signaling is necessary for the mobilization of calcium ions (Ca^{2+}) in osteoclasts in response to RANKL, we asked whether TREM2 or DAP12 could illicit Ca^{2+} flux in macrophages. Ligation of TREM2 with a specific antibody induced Ca^{2+} flux in wild-type macrophages, whereas control antibody had no effect (Fig. 2E). *SHIP1*-deficient macrophages exhibited significantly increased Ca^{2+} flux in response to stimulation of TREM2 compared to that in wild-type cells (Fig. 2E; $P = 0.123$). We examined the ability of DAP12 to recruit phospholipase C- γ 2 (PLC- γ 2), which is required for Ca^{2+} flux and osteoclastogenesis (24). Activation of TREM2 and DAP12 induced the recruitment of PLC- γ 2 to the signaling complex at 5 min (fig. S1A), at which time it also became phosphorylated (fig. S1B). Growth factor receptor-bound protein 2 (Grb2), a regulator of ERK, was also recruited to pDAP12 (fig. S1A). In summary, activation of TREM2 and DAP12 stimulated the formation of a signaling complex that consisted of intermediates that are needed for cellular activation, survival, actin reorganization, Ca^{2+} flux, and differentiation. SHIP1 was also recruited early into the complex and inhibited these effector molecules. This confirms that SHIP1 inhibits signaling intermediates downstream of TREM2 and DAP12. In the absence of SHIP1, these signals are increased in intensity and likely contribute to the enhanced differentiation of

osteoclasts and multinucleation seen in unstimulated *SHIP1*-deficient osteoclasts and in these cells after direct activation of TREM2 and DAP12.

Phosphorylation of Tyr⁶⁵ in the ITAM of DAP12 is required for the association of DAP12 with SHIP1

We next examined the molecular mechanisms that enabled the functional interaction between SHIP1 and DAP12. One possibility was that SHIP1 and DAP12 directly interacted with each other through the SH2 domain of SHIP1 and the ITAM of DAP12. Alternatively, they might interact indirectly through adaptor proteins that not only associate with SHIP1, but also contain an SH2 domain that could bind to the ITAM of DAP12. Such adaptor molecules include Grb2, Shc, Grb2-associated binding protein (GAB), and the downstream of tyrosine kinase (DOK) family members. The membrane-proximal YXXL motif in the ITAM of DAP12 is SPYQEL, and this sequence is similar to an ITIM consensus sequence that has high affinity for phosphatases (25).

To test the hypothesis that the DAP12 ITAM could bind directly to SHIP1, we made five phosphorylated peptides corresponding to the DAP12-ITAM. The ITAM of DAP12 (SPY⁶⁵QELQGQRPEVY⁷⁶SDL) contains two critical tyrosines, Tyr⁶⁵ and Tyr⁷⁶, which are needed to recruit the kinase Syk, which harbors two SH2 domains (1,26); however, SHIP1 has only one SH2 domain and potentially could bind to either of the phosphorylated tyrosines. To test the functions of Tyr⁶⁵ and Tyr⁷⁶, we generated an unphosphorylated wild-type peptide, peptides containing individual phosphorylated tyrosines (Y⁶⁵ and Y⁷⁶), a doubly phosphorylated peptide (YY), and a peptide in which both tyrosines were mutated to phenylalanines (FF) (Fig. 3A). Biotinylation of these peptides enabled the pull down of peptide-associated proteins with NeutrAvidin beads. Equimolar amounts of peptides were incubated with whole-cell lysates derived from J774 cells, and the associated proteins were pulled down and analyzed by Western blotting (Fig. 3B). SHIP1 was precipitated by the doubly phosphorylated ITAM peptide (YY) and the peptide that was singly phosphorylated at Tyr⁶⁵ (Y⁶⁵), in the putative ITIM, whereas SHIP1 was not precipitated by the wild-type unphosphorylated peptide, the Y⁷⁶ peptide, or by the mutant peptide that lacked both tyrosine residues (Fig. 3B). As a positive control for peptide binding, we analyzed Syk by Western blotting and found that it was associated with the YY and Y⁶⁵ peptides, consistent with previous studies (27,28). Our results demonstrated that SHIP1 bound to DAP12 in a manner that requires phosphorylation of the ITAM tyrosine within the sequence SPYQEL. These results are consistent with there being a direct interaction between SHIP1 and DAP12, but they do not exclude the possibility that an ITAM-binding adaptor protein may bridge these proteins.

The SH2 domain of SHIP1 is required for its binding to DAP12

We next addressed whether the SH2 domain of SHIP1 mediated its binding to DAP12. We generated glutathione *S*-transferase (GST) fusion proteins containing the isolated SH2 domain of SHIP1 (Fig. 3C) (29). An Arg³⁴→Gly substitution within the SH2 domain was generated to disrupt its binding to the ITAM (Fig. 3C) (29). To detect direct interactions between the fusion proteins containing the SHIP1 SH2 domains and the peptides containing the DAP12 ITAM, GST-fusion proteins were purified and incubated with the biotinylated ITAM peptides in lysis buffer in the absence of cell lysates. NeutrAvidin precipitates were analyzed by Western blotting with an antibody against GST to detect SH2 fusion proteins that had coprecipitated with the biotinylated ITAM peptides (Fig. 3D). The unphosphorylated wild-type ITAM peptide failed to associate with any of the fusion proteins, whereas the phosphorylated ITAM peptide Y⁶⁵ pulled down the purified GST-SH2 protein (Fig. 3D). The mutant GST-SH2 protein (mSH2) was unable to associate with the Y⁶⁵ peptide, indicating that an intact SH2 domain was needed to associate with the DAP12 ITAM. Purified GST-fusion proteins served as

positive Western blotting controls and confirmed that equal amounts of fusion protein were added to the pull-down assays (Fig. 3D).

Together, our results reveal a previously uncharacterized association of SHIP1 with DAP12 that was induced by the ligation of TREM2 and the activation of DAP12 in BMMs and osteoclasts. Direct protein-protein interactions between the SH2 domain of SHIP1 and the ITAM of DAP12 were required for this association.

The phosphatidylinositol 3-kinase regulatory subunit p85 associates with DAP12 in response to ligation of TREM2

We then investigated the mechanism by which SHIP1 inhibited signaling downstream of DAP12. Because SHIP1 is typically recruited in response to the production of phosphatidylinositol-3,4,5-trisphosphate (PIP₃) by PI3K, we hypothesized that phosphatidylinositol 3-kinase (PI3K) was activated in response to the ligation of TREM2, possibly by Syk, which would lead to the increased formation of PIP₃ and the recruitment of plextrin homology (PH) domain-containing proteins, including Akt and Vav3, to the plasma membrane. To test this hypothesis, we used an antibody against pDAP12 to perform immunoprecipitations with lysates from wild-type and *SHIP1*-deficient BMMs. Immunoprecipitates were analyzed by Western blotting for the presence of the p85 regulatory subunit of PI3K (30). Ligation of TREM2 induced the recruitment of p85 to DAP12 within 2 min in wild-type BMMs (Fig. 4A), which was not seen in cells treated with the control antibody. Furthermore, the association of p85 with DAP12 was increased in BMMs from *SHIP1*-deficient mice, compared to those from wild-type mice, confirming that SHIP1 inhibited the recruitment of p85 to the DAP12 signaling complex.

The p85 subunit of PI3K contains two SH2 domains and binds to the ITAM of the Fc receptor γ (FcR γ) chain in response to the activation of the collagen receptor complex in platelets (31). Thus, we determined whether the individual DAP12 ITAM phosphopeptides could associate with p85 (Fig. 4B). Cell lysates from wild-type BMMs were incubated with the DAP12 ITAM peptides described earlier (Fig. 3A). DAP12 ITAM phosphopeptides, including Y⁶⁵, Y⁷⁶, and YY, coimmunoprecipitated with p85, whereas the wild-type and FF mutant peptides did not (Fig. 4B). These results indicate that p85 associated with DAP12 in a phospho-ITAM-specific manner.

It remained possible that another adaptor protein might mediate the association between p85 and DAP12. One such candidate is the transmembrane adaptor, DAP10, which is closely related to DAP12; however, unlike DAP12, DAP10 contains a YINM motif that binds to p85 (32). DAP10 associates with some DAP12-associated receptors, although an association with TREM2 has not yet been reported (33,34). Therefore, we stimulated TREM2 in wild-type and *DAP10*-deficient BMMs and subjected samples to immunoprecipitation with an antibody against pDAP12. Unlike in wild-type BMMs, ligation of TREM2 failed to induce substantial recruitment of p85 and Grb2 to pDAP12 in *DAP10*-deficient cells (Fig. 4C). Analysis of whole-cell lysates revealed that stimulation of TREM2 in *DAP10*-deficient cells led to a substantially reduced activation of Akt and ERK compared to that in wild-type cells (Fig. 4D).

To further explore the association between DAP12 and DAP10, we performed immunoprecipitations with antibodies against DAP12 or DAP10 and analyzed both proteins and TREM2 by Western blotting. Both antibodies coimmunoprecipitated TREM2 (Fig. 4E). Complexes immunoprecipitated with an antibody against DAP10 were examined by reducing (fig. S2A) and nonreducing gel electrophoresis, which revealed the presence of DAP10 and DAP12 (fig. S2B). Likewise, two different antibodies against DAP12 immunoprecipitated DAP10 monomers (fig. S2A). Under nonreducing electrophoresis, which enabled disulfide bonds to be retained, we identified an approximate 20-kD band in the immunoprecipitates with

the antibody against DAP10 that reacted with both the antibody against DAP12 and the antibody against DAP10 (fig. S2B). This band may represent heterodimers of DAP12 and DAP10.

To ensure that the decreased signaling observed in *DAP10*-deficient cells was not because of a reduction in the abundance of TREM2, we examined the amount of TREM2 at the cell surface by flow cytometry. We detected equivalent amounts of TREM2 protein on the surface of wild-type and *DAP10*-deficient BMMs (fig. S3B). Finally, we performed Ca^{2+} flux studies in *DAP10*-deficient BMM and found that they had similar responses to the ligation of TREM2 as did wild-type cells (fig. S3A). These results indicated that DAP10 mediated the recruitment of p85 to DAP12 and the subsequent activation of Akt and ERK but that DAP10 was not required for DAP12-mediated Ca^{2+} flux.

We then asked whether the TREM2-dependent recruitment of p85 to the DAP12 signaling complex and the activation of Akt could alter apoptosis in osteoclasts. We induced apoptosis in bone marrow–derived osteoclasts by starving the cells of serum overnight in the presence of an antibody against TREM2, a control antibody, RANKL, or phosphate-buffered saline (PBS), as a negative control. Cell lysates were analyzed by Western blotting for the presence of myeloid cell leukemia sequence 1 (MCL-1), an anti-apoptotic protein from the B cell lymphoma/leukemia 2 (Bcl-2) family (35). Ligation of TREM2 stimulated an increase in the abundance of MCL-1 protein in wild-type and *SHIP1*-deficient osteoclasts (fig. S4A). The abundance of MCL-1 in unstimulated *SHIP1*-deficient cells was greater than that in wild-type cells, consistent with the prolonged survival of *SHIP1*-deficient cells (fig. S4A). Parallel cultures were fixed, and apoptotic cells were identified by terminal deoxynucleotidyl transferase-mediated deoxyuridine triphosphate nick end labeling (TUNEL) staining. Compared to that in cells treated with PBS or control antibody, ligation of TREM2 in wild-type and *SHIP1*-deficient osteoclast cultures substantially prevented the apoptosis of osteoclast cultures equivalent to that of RANKL (fig. S4B). Thus, ligation of TREM2 activated survival signals, including Akt, and induced the production of MCL-1, which led to the suppression of apoptosis.

PI3K activity is not required for the recruitment of SHIP1 to DAP12

We hypothesized that the recruitment of SHIP1 to DAP12 after the ligation of TREM2 required the activation of Syk or PI3K. Thus, we examined the effects of the PI3K inhibitor wortmannin on the recruitment of SHIP1 to DAP12. Unexpectedly, wortmannin enhanced the recruitment of SHIP1 to DAP12 after the ligation of TREM2 in J774 cells (Fig. 5A). The activation of Akt and Vav3 downstream of the stimulation of TREM2 was reduced (Fig. 5A), thus confirming that wortmannin inhibited the activity of PI3K. Additionally, wortmannin blocked the recruitment of p85 to DAP12 (Fig. 5A), indicating that PI3K activity was necessary for the initial association of p85 with DAP12 or to stabilize the association, possibly through a PH domain–containing protein. Surprisingly, phosphorylation of Syk, downstream of DAP12, was also inhibited by wortmannin (Fig. 5A), suggesting that Syk was downstream of PI3K after stimulation of TREM2 and DAP12. We also tested another PI3K inhibitor, LY294002, the Src inhibitor PP2, and the Syk inhibitor BAY 61-3606. Treatment of cells with LY294002 during TREM2 ligation increased the association of SHIP1 with DAP12, compared to that in control cells; however, inhibition of Src or Syk had no substantial effect on the recruitment of SHIP1 despite the decrease in the abundance of pDAP12 observed in PP2-treated cells (fig. S5A). These data suggest that in the presence of wortmannin, the extent of the binding of SHIP1 to DAP12 was increased and that this served to block other SH2 domain–containing proteins, such as Syk, Grb2, and p85, from binding to the DAP12 ITAM. Wortmannin failed to inhibit the TREM2-dependent phosphorylation of SHIP1, which indicates that this event was PI3K-

independent. Furthermore, inhibition of the activity of PI3K prevented the recruitment of Grb2 to DAP12.

We then determined the role of DAP10 in the recruitment of SHIP1 to the TREM2-DAP12 complex. Stimulation of TREM2 induced the recruitment of SHIP1 to DAP12 in *DAP10*-deficient BMMs, which indicated that DAP10 was not required for this translocation event (fig. S5B). Likewise, *DAP10*-deficient BMMs treated with wortmannin during TREM2 ligation also exhibited increased recruitment of SHIP1 to DAP12, relative to that in wild-type cells. As expected, wortmannin inhibited the activation of Akt and ERK in response to the stimulation of TREM2 (fig. S5B). These results indicated that neither DAP10 nor PI3K activity was required for the association of SHIP1 with DAP12 in response to ligation of TREM2.

Overall, these data showed that inhibition of PI3K during ligation of TREM2 favored the prolonged phosphorylation of SHIP1 and its stable recruitment to DAP12. Activated PI3K was required for the activation of Syk and the increased recruitment of p85 and Grb2 to the DAP12-associated signaling complex. However, some constitutive association of p85 with DAP10 and DAP12 was present even in the presence of wortmannin (fig. S5B). These results indicated that PI3K activity was not required to recruit the inhibitory protein SHIP1 to DAP12, whereas PI3K activity was needed for the activation of Syk and Grb2.

The association of DAP12 with p85 is regulated by SHIP1

Next, we examined whether SHIP1 regulated the TREM2-induced recruitment of p85 and Syk to the DAP12 signaling complex. BMMs derived from wild-type and *SHIP1*-deficient mice were treated with dimethyl sulfoxide (DMSO) or wortmannin together with antibody against TREM2 or control antibody. After stimulation, cell lysates were subjected to immunoprecipitations with an antibody against pDAP12, and the immunoprecipitates were examined by Western blotting for the presence of p85, Syk, Grb2, and SHIP1. Similar to data from experiments with J774 cells, wortmannin inhibited the recruitment of p85, Syk, and Grb2 to pDAP12 while increasing the association of SHIP1 with DAP12 in wild-type BMM (Fig. 5B); control antibody had no effect. In the absence of SHIP1, ligation of TREM2 induced a prolonged association among p85, Syk, Grb2, and DAP12 (Fig. 5B). These interactions were abrogated by wortmannin, confirming that PI3K activity was required to form or maintain the DAP12 signaling complex. Furthermore, wortmannin inhibited the prolonged TREM2-induced phosphorylation of Akt and ERK that was observed in *SHIP1*-deficient BMMs (Fig. 5B). These results show that stimulation of TREM2 and DAP12 induced the formation of a PI3K-dependent signaling complex that included p85, Syk, and Grb2 and that was regulated by SHIP1. Additionally, SHIP1 was recruited to the complex in a PI3K-independent manner and was required to limit the recruitment or stabilization of the DAP12 signaling complex, including the interactions between DAP12 and both p85 and Syk. These findings support a regulatory mechanism whereby the lipid phosphatase SHIP1 regulates a key immune receptor signaling complex by directly inhibiting the recruitment of PI3K.

Ligation of TREM2 induces the intracellular colocalization of SHIP1, F-actin, DAP10, and DAP12 in osteoclasts

SHIP1, DAP12, and TREM2 are implicated in the control of the cytoskeleton of osteoclasts (1,5,14,23,36,37). *SHIP1*-deficient osteoclasts are large, with increased numbers of nuclei compared to wild-type osteoclasts (23), whereas human *DAP12*- or *TREM2*-deficient osteoclasts are small and mononuclear when exposed to physiological concentrations of M-CSF (2,7,14,38). Based on these findings, we predicted that the ligation of TREM2 on serum-starved osteoclasts would lead to changes in the organization of the actin cytoskeleton and the cellular localization of SHIP1 and DAP12. To test this hypothesis, we generated BMM-derived osteoclasts from wild-type mice, which were then fixed, stained, and visualized by confocal

microscopy. Serum-starved osteoclasts had limited amounts of F-actin (Fig. 6). DAP12 was localized to the cytoplasm and plasma membrane, whereas SHIP1 was cytoplasmic. Overlay analysis revealed few clusters of colocalization of DAP12 and SHIP1 near the membrane. Ligation of TREM2 for 15 min induced the organization of F-actin (Fig. 6), and SHIP1 moved to the periphery of the cells where it colocalized with F-actin and DAP12. Thus, direct activation of TREM2 and DAP12 induced the organization of the actin cytoskeleton and led to the translocation of SHIP1 to the plasma membrane. We also addressed whether SHIP1 was needed to inhibit organization of the cytoskeleton. Serum-starved, *SHIP1*-deficient cells still contained substantial amounts of F-actin (Fig. 6), and DAP12 and F-actin colocalized in these resting cells. After stimulation of TREM2, the cells became more widely spread and DAP12 colocalized with actin in clusters along the plasma membrane. This result confirms the role of SHIP1 as an inhibitor of TREM2- and DAP12-induced cytoskeletal organization in osteoclasts.

We next examined the recruitment of SHIP1 to the membrane in the absence of DAP12. Stimulation of TREM2 failed to induce the translocation of SHIP1 from the cytoplasm to the membrane in osteoclasts derived from mice deficient in both DAP12 and FcR γ (fig. S6). Stimulation of TREM2 induced the localization of DAP10 to the plasma membrane in cap-like structures. These caps tended to colocalize with SHIP1 and F-actin in stimulated wild-type cells, but failed to do so in stimulated *DAP12*-deficient cells. This indicated that DAP12 was needed for the translocation of SHIP1 and DAP10 to actin after the stimulation of TREM2.

We then investigated whether DAP12 and SHIP1 exhibited normal trafficking in *DAP10*-deficient osteoclasts. Resting *DAP10*-deficient cells had increased amounts of F-actin compared to that in resting wild-type cells, similar to what was observed in resting *SHIP1*-deficient and TREM2-activated wild-type cells (fig. S7). Although wild-type and *DAP10*-deficient cells exhibited a similar cytoplasmic localization of DAP12 and SHIP1 at rest, SHIP1 was also found at the plasma membrane in some *DAP10*-deficient cells. After ligation of TREM2, additional SHIP1 and DAP12 translocated to the cell periphery and colocalized with F-actin in *DAP10*-deficient cells. Thus, DAP10 was not needed for the translocation of SHIP1 and DAP12 to the plasma membrane.

The costimulation of DAP12 by M-CSF and RANKL differentially recruits SHIP1 to DAP12

Thus far, we had demonstrated that SHIP1 directly inhibited TREM2 and DAP12 signaling. We next investigated whether SHIP1 regulated the costimulation of DAP12 in response to physiological stimulation of osteoclasts. We and others showed that TREM2 and DAP12 participate in osteoclast differentiation induced by M-CSF and RANKL (1–3,7,14,36,38,39). Additionally, previous studies showed that the ITAM of DAP12 is required for normal osteoclast differentiation in response to RANKL and for M-CSF-induced cell spreading (1–3,38). Indeed, M-CSF and RANKL independently lead to the phosphorylation of DAP12 through inside-out signaling (3,5). We investigated whether inside-out activation of DAP12 by M-CSF and RANKL recruited SHIP1 to DAP12. RAW 264.7 preosteoclast macrophages were treated with control medium or with medium containing M-CSF (20 ng/ml), RANKL (50 ng/ml), or both for 3 days to induce osteoclastogenesis. Cells were then lysed on the plate and lysates were used in immunoprecipitation reactions with an antibody against DAP12. SHIP1 and DAP12 coimmunoprecipitated in these adherent macrophages and osteoclasts in the absence of the cross-linking of TREM2 (Fig. 7A). This constitutive association between SHIP1 and DAP12 was likely due to a combination of the activation of DAP12 through integrins, M-CSF receptor RANK, and an unknown endogenous ligand of TREM2 found in the macrophage cultures.

To study the role of M-CSF- and RANKL-induced translocation of SHIP1 to DAP12, we removed wild-type preosteoclasts (on day 3 of treatment with M-CSF and RANKL) from the plastic plates and kept them in suspension for 2 hours during serum starvation. This effectively

decreased the constitutive association of DAP12 with SHIP1 that was seen in adherent cells (Fig. 7). Suspended cells were stimulated with M-CSF (100 ng/ml), RANKL (100 ng/ml), or both or with an antibody against TREM2. Lysates were used in immunoprecipitation reactions with an antibody against pDAP12 and analyzed by Western blotting for the presence of SHIP1. M-CSF induced the recruitment of SHIP1 to DAP12 at 5 and 20 min (Fig. 7B); however, RANKL induced a weaker and later association of SHIP1 with DAP12 that was seen only after 20 min of treatment. The costimulation of preosteoclasts with both RANKL and M-CSF failed to induce an association between SHIP1 and DAP12, even after 20 min, suggesting that the inside-out activation of DAP12 by the combination of RANKL and M-CSF induced or stabilized a signaling complex different from that associated with the direct activation of TREM2 and DAP12 or with either cytokine alone.

We examined whether the dual stimulation of ligation of TREM2 together with treatment with RANKL or M-CSF would be additive or inhibitory in terms of the recruitment of SHIP1 to DAP12. Neither costimulation of cells with TREM2 and M-CSF nor TREM2 and RANKL changed the extent of recruitment of SHIP1 to DAP12 compared to that in cells that underwent ligation of TREM2 alone (Fig. 7C). These results suggested that the direct activation of TREM2 and DAP12 was dominant compared to the inside-out activation of DAP12 by M-CSF and RANKL. Additionally, these results showed that SHIP1 differentially regulated DAP12 depending on whether the cells were exposed to a combination of cytokines or to direct stimulation of TREM2.

Because our initial studies with the antibody specific for pTyr⁷⁶ in DAP12 failed to show any substantial changes in the abundance of pDAP12, we repeated these studies with an alternative antibody against pDAP12 (Ab 2426), which had less specificity for Tyr⁷⁶. Ligation of TREM2 and stimulation with M-CSF substantially increased the abundance of pDAP12 compared to that in unstimulated cells, whereas RANKL did not (Fig. 7D). Although pDAP12 was most abundant after 5 min of stimulation with M-CSF, stimulation of TREM2 induced the earlier phosphorylation of DAP12. These data support our previous finding that the phosphorylation state of DAP12 was critical for the recruitment of SHIP1.

In summary, our results show that M-CSF and RANKL individually induced the recruitment of SHIP1 to DAP12, although the kinetics of recruitment were different from those of direct stimulation of TREM2 and DAP12 by antibody. Strong osteoclastogenic stimulation with RANKL and M-CSF, however, failed to recruit SHIP1 to DAP12, perhaps as a way to amplify the converging signals without inducing an inhibitory signal. These data indicate that inside-out signaling by other physiological stimuli of osteoclasts was regulated by the association of SHIP1 with DAP12.

Inside-out signaling by M-CSF, but not RANKL, induces the colocalization of DAP12, SHIP1, and F-actin

Both M-CSF and RANKL participate in the regulation of the osteoclast cytoskeleton. Our data indicated that direct activation of DAP12 by the ligation of TREM2 induced cytoskeletal changes that were inhibited by SHIP1. We also found, however, that the combination of RANKL and M-CSF in nonadherent preosteoclasts failed to induce the recruitment of SHIP1 to DAP12 (Fig. 7B). Therefore, we asked whether M-CSF or RANKL could induce the colocalization of DAP12 with F-actin or SHIP1. Osteoclasts derived from wild-type or *SHIP1*-deficient BMMs were starved of serum for 4 hours, stimulated with either M-CSF or RANKL for 1 hour, fixed, and stained. M-CSF induced the formation of F-actin that colocalized with DAP12 (Fig. 8). SHIP1 remained cytoplasmic, and only a few punctate areas of colocalization of DAP12 and F-actin were visible at the plasma membrane (Fig. 8). DAP12 had a punctate, cytoplasmic appearance in serum-starved *SHIP1*-deficient cells, and M-CSF induced the translocation of DAP12 to the cell periphery where it colocalized with F-actin.

RANKL failed to induce the formation of F-actin or the translocation of SHIP1 to the plasma membrane. RANKL also failed to induce substantial colocalization of SHIP1, F-actin, and DAP12 in wild-type cells. *SHIP1*-deficient osteoclasts stimulated with RANKL developed a substantially altered actin cytoskeleton with punctate colocalization of DAP12 and F-actin. These data confirm that inside-out signaling by M-CSF or RANKL led to the differential recruitment of SHIP1 and DAP12 to the cell periphery, where they colocalized with F-actin.

DISCUSSION

To identify potential inhibitors of DAP12, we screened candidate phosphatases in a functional assay of osteoclast differentiation and multinucleation. We initially focused on the lipid phosphatase SHIP1 because *SHIP1*-deficient osteoclasts are highly multinucleated and well spread out, similar to osteoclasts differentiated from macrophages that overexpress either DAP12 or TREM2 (2,14). We hypothesized that loss of SHIP1 might lead to excessive TREM2 and DAP12 signaling, which would result in the formation of large, complex, highly multinucleated osteoclasts. Supporting this hypothesis, BMMs from *SHIP1*-deficient mice stimulated by the ligation of TREM2 developed fourfold more osteoclasts than did BMMs from wild-type, littermate controls, indicating that SHIP1 was needed to inhibit the stimulation of TREM2 and DAP12. We determined that the molecular mechanism of this inhibition involved the direct binding of SHIP1, through its SH2 domain, to the membrane-proximal SPYQEL sequence within the ITAM of DAP12. The recruitment of SHIP1 to DAP12 occurred early during signaling, at which point it served to limit the activation of Syk, PI3K, and ERK1/2, as well as inhibiting Ca^{2+} flux. In a similar manner, SHIP1 inhibits Fc ϵ RI γ -induced phagocytosis by binding directly to the γ -chain ITAM early during signal induction (19,20). We speculate that SHIP1 may play a similar role in regulating the phagocytosis of bacteria mediated by TREM2 and DAP12 (40).

Although much is known about DAP12 signaling in natural killer (NK) cells and neutrophils, relatively little is known about the intracellular signaling events downstream of DAP12 in macrophages, monocytes, and osteoclasts. Even less is known about the specific signaling events induced by the activation of the TREM2-DAP12 pathway. TREM2 is a unique DAP12-associated receptor, because it induces the phagocytosis of bacteria by macrophages (40), participates in the differentiation and activation of osteoclasts (14), and inhibits TLR signals in macrophages and dendritic cells (12,17). Therefore, we hypothesized that the stimulation of TREM2 and DAP12 might lead to alternative signaling pathways that could both activate and inhibit signaling in osteoclasts. Because specific endogenous ligands for TREM2 are not yet known, we activated endogenous TREM2 and DAP12 by cross-linking TREM2 with a specific monoclonal antibody. Although this approach could artificially induce nonphysiological protein-protein interactions or nonspecifically engage Fc receptors such as FcRIIb, it has been successfully used to analyze signaling events downstream of TREM1-DAP12 (41), SIRP β -DAP12 (42), and MDL-1-DAP12 (43). Indeed, by stimulating SIRP β and MDL-1 with antibodies against these receptors, we showed the differential recruitment of SHIP1 to DAP12, indicating that these results were specific for the receptors we examined.

The cross-linking of TREM2 induced the phosphorylation of Syk, ERK1/2, Akt, PLC- γ 2, and Vav3. These data demonstrate that cross-linking of TREM2 activates multiple signaling pathways involved in the control of the actin cytoskeleton (Vav3, Syk), cell survival (Akt, MCL-1), and cell differentiation and activation (PLC- γ 2, Syk, ERK1/2) (Fig. 9). Confirming the functional importance of these signaling results, we found that osteoclasts stimulated by ligation of TREM2 rapidly reorganized their cytoskeletons (which resulted in the generation of F-actin and increased multinucleation) and were resistant to serum starvation-induced apoptosis. We found that SHIP1 inhibited these events by directly binding to DAP12 and limiting the recruitment of Syk and PI3K to DAP12.

We propose a model in which dual complexes are formed after the activation of TREM2-DAP12 (Fig. 9). First, ligation of TREM2 leads to the formation of an activation complex that includes DAP10, p85, Syk, and Grb2 that results in the activation of ERK1/2, Vav, and Akt. SHIP1 becomes phosphorylated and translocates to the DAP12 complex. Upon docking with the ITAM of DAP12 at position Tyr⁶⁵, SHIP1 converts the activating signaling complex into an inhibitory one. SHIP1 prevents the additional recruitment of Syk or p85 to the signaling complex and serves to inhibit the additional activation of Akt and Vav3 and the generation of a Ca²⁺ flux. SHIP1 might also serve as an inhibitor of Tec kinases that might be activated by DAP12 signaling, thus serving to reduce the recruitment of additional p85, PLC- γ 2 activation, and Ca²⁺ flux. Additional studies are needed to determine the extent to which SHIP1 might inhibit Tec kinases downstream of DAP12.

Our data suggest that both DAP12 and DAP10 are required for the full activation of DAP12, but not for the recruitment of SHIP1. Additional studies are needed to determine the precise ratio of DAP12 to DAP10 in the TREM2 signaling complex; however, our data support the possibility that DAP10 and DAP12 could form a heterodimer that directly associates with TREM2. The normal abundance of TREM2 at the cell surface in *DAP10*-deficient cells suggests that a TREM2-DAP10 complex does not substantially contribute to the surface localization of TREM2.

DAP10-deficient mice develop age-induced osteopetrosis and exhibit decreased osteoclastogenesis in vitro, compared to that of wild-type mice (34). DAP10 forms a complex with MDL-1 and DAP12 and contributes to MDL-1–DAP12 signaling (34). Disruption of a complex containing MDL-1, DAP10, and DAP12 in *DAP10*-deficient mice was postulated to be the cause of the decreased bone remodeling in vivo and decreased osteoclastogenesis in vitro (34). Our current studies suggest two alternative mechanisms. First, we showed that SHIP1 was recruited to MDL-1. If SHIP1 and p85 regulate MDL-1–DAP12 signaling, we would expect that the absence of DAP10-mediated recruitment of p85 to DAP12 would lead to excessive recruitment of SHIP1; thus, MDL-1–DAP12 signals would be more inhibitory than activating. Second, in the absence of DAP10, TREM2-DAP12 activation signals are decreased and SHIP1 would be bound to the DAP12 ITAM, thus preventing the additional recruitment of Syk and p85. This would also lead to decreased responses to inside-out signaling by RANKL and M-CSF, which would result in decreased formation of osteoclasts in the *DAP10*-deficient cells, as has been demonstrated (34). Thus, the loss of DAP10 would partially affect several signaling pathways that are critical for osteoclastogenesis.

Finally, we propose that tonic signaling of DAP12 involves constitutive engagement of p85 and SHIP1. In the absence of SHIP1, the constitutive engagement of DAP12 with p85 leads to increased production of PIP₃ and the possible recruitment of PH domain-containing Tec kinases, which would recruit additional p85 leading to increased activation of PI3K and downstream signals. In macrophages and osteoclasts, this would lead to enhanced sensitivity to M-CSF with increased proliferation and decreased apoptosis. It would also result in increased costimulation of DAP12 with RANKL, leading to increased osteoclastogenesis. Indeed, we found that RANKL, M-CSF, and ligation of TREM2 substantially increased the differentiation and multinucleation of osteoclasts compared to that induced by control antibody with RANKL and M-CSF. These results are consistent with previous studies showing that loss of DAP12 in human and mouse osteoclasts leads to mononuclear, poorly spread osteoclasts in vitro (2,7, 38).

In addition, these results are consistent with studies showing that mutations in or deletion of the gene encoding TREM2 in human peripheral blood mononuclear cells or the mouse monocyte line RAW 264.7 leads to fewer, multinuclear osteoclasts, whereas the increased abundance of TREM2 correlates with osteoclastogenesis in vitro (7,14). Although primary

human osteoclasts lacking TREM2 or DAP12 develop into small, dysfunctional osteoclasts in vitro, primary osteoclasts from mice deficient in TREM2 have accelerated osteoclastogenesis in vitro despite exhibiting normal osteoclast function in vivo (16). Why the loss of TREM2 would lead to opposing phenotypes in human and mouse osteoclasts is still unclear. One possibility is that the TREM2-deficient mice may still produce a soluble form of TREM2 that could act as a decoy receptor for the endogenous ligand of TREM2. The blockade of TREM2 ligand by a soluble form of TREM2 could have additional influences on in vitro-derived osteoclasts that would enable accelerated differentiation. Alternatively, other DAP12-associated receptors, such as MDL-1 or SIRP β , may influence osteoclastogenesis in the absence of TREM2 in mouse, but not human osteoclasts. Here, we found that SIRP β failed to substantially recruit SHIP1 to DAP12; thus, in the absence of TREM2, stimulation of SIRP β could lead to increased DAP12 signaling without the substantial inhibition provided by SHIP1. In the absence of TREM2-mediated activation of SHIP1, accelerated osteoclastogenesis could occur because of the loss of inhibition of p85 and Syk, thus driving excessive differentiation and multinucleation. Further studies are needed to clarify these possibilities.

In addition to the activation of PLC- γ 2, Syk, and ERK1/2, TREM2-DAP12 signaling led to the recruitment of the p85 subunit of PI3K to DAP12 and the activation of Akt. Two mechanisms of p85 recruitment are supported by our data. First, p85 was coimmunoprecipitated with DAP12 pITAM peptides, which suggests a direct interaction between p85 and DAP12. Previous studies have demonstrated that p85 binds to other ITAMs including the ITAM of Fc ϵ RI γ and the ITAM in FcRIIA, the low-affinity rat immunoglobulin G (IgG) receptor, in platelets (31). Second, we showed that DAP10 formed complexes with DAP12 and provided an additional YINM PI3K-binding site. The p85 PI3K subunit constitutively bound to DAP12 in wild-type and *DAP10*-deficient cells, indicating that this may represent tonic DAP12 ITAM signaling. However, the TREM2-induced increase in the recruitment of p85 to the DAP12 complex required DAP10 and was inhibited by wortmannin. These data suggest that the recruitment of additional p85 and Syk to the DAP12 complex requires some initial generation of PIP₃, possibly leading to the recruitment of PH domain-containing proteins that are needed for stabilization of the signaling complex.

The PI3K inhibitors wortmannin and LY294002 prevented the recruitment to DAP12 of p85 and Syk but failed to inhibit the phosphorylation or translocation of SHIP1. These data suggest that PI3K is upstream of Syk after the activation of TREM2-DAP12 in BMMs and osteoclasts. This is different from DAP12 signaling in NK cells, in which Syk acts upstream of PI3K (44,45). In neutrophils, PI3K is upstream of Syk after stimulation of TLR4 by lipopolysaccharide (LPS) (46). PI3K is reported to be upstream of Syk in platelets activated by the binding of collagen to the collagen receptor (31). It remains to be determined whether this signaling pathway is unique to TREM2-DAP12 or occurs downstream of other DAP12-associated receptors in macrophages and osteoclasts.

Given the recruitment of PI3K and activation of Akt, we postulated that PI3K activity would be necessary to recruit SHIP1 to DAP12. Unexpectedly, PI3K inhibitors increased the association of DAP12 with SHIP1, as well as the extent of phosphorylation of SHIP1. One possibility for this finding is that PI3K-dependent production of PIP₃ leads to the recruitment of a PH domain-containing adaptor protein that could either sequester SHIP1 away from DAP12, participate in the recruitment of a phosphatase or an inhibitor kinase, such as Csk or Lyn, or both. DOK3 is an intriguing candidate because it binds to SHIP1, Grb2, and Csk in B cells in which it inhibits B cell antigen receptor (BCR) ITAM signaling (47–49). A second possibility is that SHIP1 and DAP12 move into or out of lipid rafts in a PI3K-dependent manner. A third possibility is that the binding of SHIP1 to Tyr⁶⁵ in the ITAM of DAP12 prevents other SH2 domain-containing proteins, such as Syk, Grb2, and p85, from binding to the ITAM. Studies are under way to differentiate among these possibilities.

We found that SHIP1 was differentially recruited to DAP12 through inside-out signaling downstream of RANKL and M-CSF. During strong stimulation of osteoclasts with RANKL alone or with RANKL and M-CSF, SHIP1 was not recruited to DAP12, which indicates that this combination of cytokines may induce an “activation”-only signal that is needed to sustain Ca^{2+} flux, activate the transcription factor nuclear factor of activated T cells (NFAT), and drive osteoclastogenesis; however, M-CSF induced the association of DAP12 with SHIP1 and revealed another avenue by which SHIP1 could inhibit M-CSF signaling.

In summary, we have identified a previously uncharacterized, direct association of SHIP1 with DAP12 that was necessary to inhibit TREM2- and DAP12-dependent signaling in macrophages and osteoclasts. These studies confirm that TREM2 and DAP12 are critical regulators of osteoclast cytoskeletal changes and multinucleation. Furthermore, they reveal the complexity of inside-out signaling of DAP12 by RANKL and M-CSF. Given these results, we propose that the large, highly multinuclear osteoclasts and the severe osteoporotic phenotype of *SHIP1*-deficient mice is due, in part, to excessive and prolonged DAP12 signaling that results from both direct stimulation of TREM2, as well as inside-out signaling by RANKL and M-CSF. The defect in osteoblast maturation identified in *SHIP1*-deficient mice may also contribute to the osteoporotic defect in these mice (50). We conclude that TREM2 and DAP12 are critical regulators of osteoclasts and that SHIP1-mediated inhibition of TREM2- and DAP12-dependent ITAM-induced signaling is required to prevent the uncontrolled activation and survival of osteoclasts.

This work also has broader implications for the regulation of inositol phospholipid signaling. Here, we identified a mechanism for the regulation of PI3K by SHIP1 that occurs by the docking of SHIP1 at an immunoreceptor ITAM, which directly prevented the recruitment of PI3K to the signaling complex. This mechanism may be particularly important for regulation of tonic ITAM signals or to facilitate the generation of inhibitory signals that are needed to prevent excessive innate immune responses. Identification of endogenous ligands for TREM2 and other DAP12-associated receptors will enable further delineation of these possibilities.

MATERIALS AND METHODS

Animals

SHIP1^{-/-} mice (on a C57BL/6 background) were provided by G. Krystal by way of K. M. Coggeshall [Oklahoma Medical Research Foundation (OMRF)]. Heterozygous mice were bred, and animals were genotyped on postnatal day 15. Wild-type (WT) littermates were used as controls. Mice doubly deficient in *DAP12* and *FcR γ* were provided by R. McEver (OMRF). *DAP10*-deficient bone marrow was provided by L. Lanier [University of California San Francisco (UCSF)]. Animals were maintained according to the guidelines of the Association for Assessment and Accreditation of Laboratory Animal Care at the OMRF.

Reagents and antibodies

Antibody against SHIP1 (P1C1) and polyclonal antibodies against DAP12 and Syk (N-19) were obtained from Santa Cruz Biotechnology; antibodies against ERK (panERK) and pERK (pThr²⁰²/pTyr²⁰⁴), and purified rat IgG1 (κ monoclonal immunoglobulin isotype) were from BD Transduction Laboratories; antibodies against Akt (pan) C67E7, pAkt (Thr³⁰⁸) C31E5, Grb2, and PLC- γ 2 were obtained from Cell Signaling Technology, antibody against Vav3 was from Abcam; antibody against p85 was a gift from K. Mark Coggeshall; antibody against DAP12 was a gift from Takai (Tohoku University, Japan); the 4G10-agarose conjugate was from Upstate Biotechnology. Rat antibody against TREM2 (clone 78) was previously described (14) and was generously provided by W. E. Seaman (UCSF). In conjunction with Epitomics, we generated rabbit polyclonal antibodies against pDAP12 (2425 and 2426) by

injecting rabbits with the peptide CGRPEVpYSDLNTQR-amide. All fluorescently-conjugated secondary antibodies were purchased from Invitrogen. Murine M-CSF and RANKL were obtained from Peprotech. Wortmannin was obtained from Calbiochem.

Culture of macrophage cell lines

RAW 264.7 and J774 cells were obtained from the American Type Culture Collection. The cells were maintained in complete medium [α -minimal essential medium (α -MEM) supplemented with 10% fetal calf serum (FCS), 2 mM L-glutamine, penicillin (100 U/ml), and streptomycin (100 μ g/ml)].

Culture of BMMs and osteoclastogenesis

All procedures were performed essentially as described earlier (2). Briefly, bone marrow cells were flushed from femurs and tibias with a 25-gauge needle. Red blood cells (RBCs) were lysed with RBC lysis buffer [0.16 M NH_4Cl , 0.17 M tris (pH 7.65)] for 3 min at room temperature, and washed with PBS. Cells were cultured in complete α -MEM supplemented with 10% fetal bovine serum, 1% glutamine Pen-Strep, and M-CSF (10 to 20 ng/ml; Peprotech). After 2 days in culture with M-CSF, nonadherent BMMs were transferred to new plates at a density of 100,000 cells per well for a 96-well plate, 250,000 cells per well in a 24-well plate, 1×10^6 cells per well in Permanox chamber slides, or 5×10^6 cells per 10-cm dish. BMMs were cultured for an additional 2 to 5 days with M-CSF. Preosteoclasts and osteoclasts were derived from BMMs in complete α -MEM with RANKL (25 ng/ml) and M-CSF (10 ng/ml) for an additional 3 to 5 days.

Stimulation of cells, immunoprecipitation reactions, and Western blotting

Cells (J774, RAW 264.7, BMMs, or osteoclasts) were removed from tissue culture dishes with PBS-EDTA, washed with PBS, and counted. J774 (40×10^6) or RAW 264.7 cells (10×10^6 BMM or osteoclasts) were incubated with antibody against TREM2 or with isotype-matched control antibody at $1 \mu\text{g}/10^6$ cells for 20 min on ice followed by cross-linking with antibody against rat IgG F(ab')₂ for the times indicated in the figure legends. Cells were lysed in ice-cold radioimmunoprecipitation assay (RIPA) buffer [50 mM tris-HCl (pH 7.4), 150 mM NaCl, 1 mM EDTA, 1% Triton-100, 1 mM NaF, 1 mM phenylmethylsulfonyl fluoride, 1 mM Na_3VO_4 , 0.25% sodium deoxycholate, aprotinin (1 $\mu\text{g}/\text{ml}$), leupeptin (1 $\mu\text{g}/\text{ml}$), pepstatin (1 $\mu\text{g}/\text{ml}$)] for 20 min followed by centrifugation at 16,000g for 10 min at 4°C to remove insoluble materials. The resulting supernatants were subjected to immunoprecipitation reactions with the indicated antibodies and protein A- or protein G-agarose (Sigma). The beads were extensively washed with RIPA buffer and the proteins were separated by SDS-polyacrylamide gel electrophoresis (SDS-PAGE). The proteins were transferred to nitrocellulose membranes by Western blotting, incubated with the appropriate antibodies, and visualized with the enhanced chemiluminescence (ECL) system (Pierce).

Generation of GST-SHIP-SH2 and GST-SHIP-SH2(R34G) proteins

The SH2 domain of SHIP1 spans amino acid residues 5 to 105. The complementary DNA (cDNA) encoding this fragment was amplified from pcDNA3.1 containing mouse *SHIP1* (provided by K. Mark Coggeshall). SHIP1 (R34G), an SH2 domain mutant, was generated with the QuikChange Site-Directed Mutagenesis kit (Stratagene). The polymerase chain reaction products were inserted into pGEX-3X between the Eco RI and Bam HI sites and sequenced. Expression of the fusion proteins in cultures of transformed *Escherichia coli* was induced with isopropyl- β -D-thiogalactopyranoside. Fusion proteins were purified with glutathione-agarose (Sigma), and analyzed by SDS-PAGE and Western blotting with antibody against GST.

In vitro peptide pull-down assays

The in vitro peptide assays were based on methods previously described (29,51,52). Biotinylated WT, phosphorylated, and mutant DAP12 ITAM peptides with the core sequence of SPYQELQGQRPEVYSDL (Fig. 3A) were synthesized by Quality Controlled Biochemicals. Whole-cell lysates were incubated with biotinylated peptides overnight at 4°C with rotation. Peptides and associated proteins were collected with NeutrAvidin-Sepharose (Pierce), washed with RIPA buffer, and subjected to SDS-PAGE and Western blotting analysis. In other assays, biotinylated peptides were added to purified, recombinant GST-SHIP SH2 or mutant SH2 proteins in RIPA buffer for 4 hours at 4°C. Peptide-associated proteins were collected and processed as described earlier. Western blot membranes were incubated with antibody against GST to detect GST-fusion proteins that were pulled down with the peptides.

Immunofluorescence confocal microscopy

BMMs were cultured in eight-well Permanox chamber slides in the presence of RANKL (50 ng/ml) and M-CSF (10 ng/ml) to generate small, multinucleated osteoclasts. After 3 days, the medium was changed to serum-free medium for 2 to 4 hours before stimulation with M-CSF (100 ng/ml), RANKL (100 ng/ml), or antibody against TREM2 (as described earlier) for 1 hour at 37°C. Cells were fixed with 1 to 2% paraformaldehyde and permeabilized with 0.05% saponin in PBS for 30 min at room temperature. After being blocked with antibody (2.4G2) for 1 hour at room temperature, the slides were incubated with goat polyclonal antibody against DAP12, rabbit antibody against SHIP1 (Santa Cruz Biotechnologies), or both overnight at 4°C. Cells were washed with PBS and incubated for 1 hour at room temperature with fluorescein isothiocyanate (FITC)-conjugated donkey antibody against rabbit IgG, CY3-conjugated donkey antibody against goat IgG (both from Jackson ImmunoResearch), and Alexa Fluor 647 phalloidin (Invitrogen). Samples were viewed with a Zeiss LSM510 confocal microscope (OMRF). The images were analyzed with LSM confocal software.

Osteoclast differentiation assays

To stimulate TREM2 during osteoclastogenesis, 96-well plates were coated overnight at 4°C with monoclonal antibody against TREM2 (20 µg/ml) or an isotype-matched control monoclonal antibody (R35-95, BD Biosciences). BMMs were seeded onto the plates in triplicate wells and treated with RANKL and M-CSF as described earlier. The medium was changed every 3 days until large multinucleated cells were visible. After 3 to 5 days in culture, cells were fixed with 3.7% formaldehyde in PBS for 10 min. Plates were then washed twice in PBS, incubated for 30 s in a solution of 50% acetone and 50% ethanol, and washed with PBS. Cells were stained for tartrate-resistant acid phosphatase (TRAP) with a kit from Sigma (product 435). Multinucleated (more than two nuclei), TRAP-positive cells were then counted by light microscopy.

Apoptosis assays

Mature osteoclast cultures were differentiated in 24-well dishes with RANKL and M-CSF. After 4 days, complete medium was substituted with serum-free medium to induce apoptosis. Cells were treated with RANKL, PBS, antibody against TREM2, or an isotype-matched control antibody during the overnight serum starvation. Cells were fixed in 1% paraformaldehyde and stained with a TUNEL-based kit (Millipore Corporation) according to the manufacturer's instructions. Apoptotic nuclei were counted with a Nikon TE2000-E microscope with 20× magnification. Results are expressed as the percentage of apoptotic cells relative to the total number of cells in six randomly selected fields of the two wells.

Ca²⁺ flux assays

BMMs were washed twice with Hepes-containing buffer [20 mM Hepes (pH 7.3), 120 mM NaCl, 1 mM CaCl₂, 1 mM MgCl₂, 5 mM KCl, glucose (1 mg/ml), bovine serum albumin (1 mg/ml)] followed by incubation in 0.05% Pluronic F-127 (Invitrogen) and 1 μM Indo-1 AM (Invitrogen) for 20 min at 37°C. Cells were washed twice with Hepes buffer and were then stimulated with antibody against TREM2 or with control antibody (16 μg/ml) and monitored by spectrophotometer (PTL Photon Technology International). The Indo-1 fluorescence emission was converted to [Ca²⁺] according to the manufacturer's instructions.

Statistical analysis

Statistical analyses were performed with GraphPad Prism Plus software. Three or more comparisons were analyzed by one way analysis of variance (ANOVA). Studies with two comparisons were analyzed with the Student's *t* test.

Supplementary Material

Refer to Web version on PubMed Central for supplementary material.

Acknowledgments

We thank M. Nakamura, B. Seaman, and L. Lanier for their critical review of the data and the manuscript. Antibodies against TREM2 were provided by B. Seaman and M. Nakamura. We thank L. Lanier and M. Orr for providing DAP10-deficient bone marrow and T. Takai for providing antiserum specific for DAP12.

This work was supported by Department of Veteran's Affairs grants to M.B.H., NIH grants to M.B.H. (DE019398, P20 RR0201143), W.G.K. (HL085580, HL72523), by the Paige Arnold Butterfly Run grant to W.G.K., and by grant U19 AI062629 to K.M.C.

REFERENCES AND NOTES

- Mócsai A, Humphrey MB, Van Ziffle JA, Hu Y, Burghardt A, Spusta SC, Majumdar S, Lanier LL, Lowell CA, Nakamura MC. The immunomodulatory adapter proteins DAP12 and Fc receptor γ-chain (FcRγ) regulate development of functional osteoclasts through the Syk tyrosine kinase. *Proc Natl Acad Sci USA* 2004;101:6158–6163. [PubMed: 15073337]
- Humphrey MB, Ogasawara K, Yao W, Spusta SC, Daws MR, Lane NE, Lanier LL, Nakamura MC. The signaling adapter protein DAP12 regulates multinucleation during osteoclast development. *J Bone Miner Res* 2004;19:224–234. [PubMed: 14969392]
- Koga T, Inui M, Inoue K, Kim S, Suematsu A, Kobayashi E, Iwata T, Ohnishi H, Matozaki T, Kodama T, Taniguchi T, Takayanagi H, Takai T. Costimulatory signals mediated by the ITAM motif cooperate with RANKL for bone homeostasis. *Nature* 2004;428:758–763. [PubMed: 15085135]
- Nataf S, Anginot A, Vuaillet C, Malaval L, Fodil N, Chereul E, Langlois JB, Dumontel C, Cavillon G, Confavreux C, Mazzorana M, Vico L, Belin MF, Vivier E, Tomasello E, Jurdic P. Brain and bone damage in KARAP/DAP12 loss-of-function mice correlate with alterations in microglia and osteoclast lineages. *Am J Pathol* 2005;166:275–286. [PubMed: 15632019]
- Zou W, Reeve JL, Liu Y, Teitelbaum SL, Ross FP. DAP12 couples c-Fms activation to the osteoclast cytoskeleton by recruitment of Syk. *Mol Cell* 2008;31:422–431. [PubMed: 18691974]
- Zou W, Kitaura H, Reeve J, Long F, Tybulewicz VL, Shattil SJ, Ginsberg MH, Ross FP, Teitelbaum SL. Syk, c-Src, the αvβ3 integrin, and ITAM immunoreceptors, in concert, regulate osteoclastic bone resorption. *J Cell Biol* 2007;176:877–888. [PubMed: 17353363]
- Paloneva J, Mandelin J, Kiialainen A, Bohling T, Prudlo J, Hakola P, Haltia M, Kontinen YT, Peltonen L. DAP12/TREM2 deficiency results in impaired osteoclast differentiation and osteoporotic features. *J Exp Med* 2003;198:669–675. [PubMed: 12925681]

8. Wu Y, Torchia J, Yao W, Lane NE, Lanier LL, Nakamura MC, Humphrey MB. Bone microenvironment specific roles of ITAM adapter signaling during bone remodeling induced by acute estrogen-deficiency. *PLoS One* 2007;2:e586. [PubMed: 17611621]
9. Lanier LL. DAP10- and DAP12-associated receptors in innate immunity. *Immunol Rev* 2009;227:150–160. [PubMed: 19120482]
10. Turnbull IR, Gilfillan S, Cella M, Aoshi T, Miller M, Piccio L, Hernandez M, Colonna M. Cutting edge: TREM-2 attenuates macrophage activation. *J Immunol* 2006;177:3520–3524. [PubMed: 16951310]
11. Hamerman JA, Tchao NK, Lowell CA, Lanier LL. Enhanced Toll-like receptor responses in the absence of signaling adaptor DAP12. *Nat Immunol* 2005;6:579–586. [PubMed: 15895090]
12. Hamerman JA, Jarjoura JR, Humphrey MB, Nakamura MC, Seaman WE, Lanier LL. Cutting edge: Inhibition of TLR and FcR responses in macrophages by triggering receptor expressed on myeloid cells (TREM)-2 and DAP12. *J Immunol* 2006;177:2051–2055. [PubMed: 16887962]
13. Hamerman JA, Lanier LL. Inhibition of immune responses by ITAM-bearing receptors. *Sci STKE* 2006;2006:re1. [PubMed: 16449667]
14. Humphrey MB, Daws MR, Spusta SC, Niemi EC, Torchia JA, Lanier LL, Seaman WE, Nakamura MC. TREM2, a DAP12-associated receptor, regulates osteoclast differentiation and function. *J Bone Miner Res* 2006;21:237–245. [PubMed: 16418779]
15. Turnbull IR, Gilfillan S, Cella M, Aoshi T, Miller M, Piccio L, Hernandez M, Colonna M. Cutting Edge: TREM-2 attenuates macrophage activation. *J Immunol* 2006;177:3520–3524. [PubMed: 16951310]
16. Colonna M, Turnbull I, Klesney-Tait J. The enigmatic function of TREM-2 in osteoclastogenesis. *Adv Exp Med Biol* 2007;602:97–105. [PubMed: 17966394]
17. Chu CL, Yu YL, Shen KY, Lowell CA, Lanier LL, Hamerman JA. Increased TLR responses in dendritic cells lacking the ITAM-containing adapters DAP12 and FcR γ . *Eur J Immunol* 2008;38:166–173. [PubMed: 18081038]
18. Coggeshall KM, Nakamura K, Phee H. How do inhibitory phosphatases work? *Mol Immunol* 2002;39:521–529. [PubMed: 12431385]
19. Nakamura K, Malykhin A, Coggeshall KM. The Src homology 2 domain-containing inositol 5-phosphatase negatively regulates Fc γ receptor-mediated phagocytosis through immunoreceptor tyrosine-based activation motif-bearing phagocytic receptors. *Blood* 2002;100:3374–3382. [PubMed: 12384440]
20. Maresco DL, Osborne JM, Cooney D, Coggeshall KM, Anderson CL. The SH2-containing 5'-inositol phosphatase (SHIP) is tyrosine phosphorylated after Fc γ receptor clustering in monocytes. *J Immunol* 1999;162:6458–6465. [PubMed: 10352260]
21. Pasquier B, Launay P, Kanamaru Y, Moura IC, Pfirsch S, Ruffié C, Hénin D, Benhamou M, Pretolani M, Blank U, Monteiro RC. Identification of Fc α RI as an inhibitory receptor that controls inflammation: Dual role of FcR γ ITAM. *Immunity* 2005;22:31–42. [PubMed: 15664157]
22. Hesslein DG, Takaki R, Hermiston ML, Weiss A, Lanier LL. Dysregulation of signaling pathways in CD45-deficient NK cells leads to differentially regulated cytotoxicity and cytokine production. *Proc Natl Acad Sci USA* 2006;103:7012–7017. [PubMed: 16627620]
23. Takeshita S, Namba N, Zhao JJ, Jiang Y, Genant HK, Silva MJ, Brodt MD, Helgason CD, Kalesnikoff J, Rauh MJ, Humphries RK, Krystal G, Teitelbaum SL, Ross FP. SHIP-deficient mice are severely osteoporotic due to increased numbers of hyper-resorptive osteoclasts. *Nat Med* 2002;8:943–949. [PubMed: 12161749]
24. Mao D, Epple H, Uthgenannt B, Novack DV, Faccio R. PLC γ 2 regulates osteoclastogenesis via its interaction with ITAM proteins and GAB2. *J Clin Invest* 2006;116:2869–2879. [PubMed: 17053833]
25. Burshtyn DN, Lam AS, Weston M, Gupta N, Warmerdam PA, Long EO. Conserved residues amino-terminal of cytoplasmic tyrosines contribute to the SHP-1-mediated inhibitory function of killer cell Ig-like receptors. *J Immunol* 1999;162:897–902. [PubMed: 9916713]
26. Johnson SA, Pleiman CM, Pao L, Schneringer J, Hippen K, Cambier JC. Phosphorylated immunoreceptor signaling motifs (ITAMs) exhibit unique abilities to bind and activate Lyn and Syk tyrosine kinases. *J Immunol* 1995;155:4596–4603. [PubMed: 7594458]

27. Kimura T, Sakamoto H, Appella E, Siraganian RP. Conformational changes induced in the protein tyrosine kinase p72syk by tyrosine phosphorylation or by binding of phosphorylated immunoreceptor tyrosine-based activation motif peptides. *Mol Cell Biol* 1996;16:1471–1478. [PubMed: 8657120]
28. de Mol NJ, Catalina MI, Dekker FJ, Fischer MJ, Heck AJ, Liskamp RM. Protein flexibility and ligand rigidity: A thermodynamic and kinetic study of ITAM-based ligand binding to Syk tandem SH2. *Chembiochem* 2005;6:2261–2270. [PubMed: 16252296]
29. Tridandapani S, Kelley T, Pradhan M, Cooney D, Justement LB, Coggeshall KM. Recruitment and phosphorylation of SH2-containing inositol phosphatase and Shc to the B-cell Fc γ immunoreceptor tyrosine-based inhibition motif peptide motif. *Mol Cell Biol* 1997;17:4305–4311. [PubMed: 9234687]
30. Jacob A, Cooney D, Tridandapani S, Kelley T, Coggeshall KM. Fc γ RIIb modulation of surface immunoglobulin-induced Akt activation in murine B cells. *J Biol Chem* 1999;274:13704–13710. [PubMed: 10224144]
31. Gibbins JM, Bridson S, Shutes A, van Vugt MJ, van de Winkel JG, Saito T, Watson SP. The p85 subunit of phosphatidylinositol 3-kinase associates with the Fc receptor γ -chain and linker for activator of T cells (LAT) in platelets stimulated by collagen and convulxin. *J Biol Chem* 1998;273:34437–34443. [PubMed: 9852111]
32. Billadeau DD, Upshaw JL, Schoon RA, Dick CJ, Leibson PJ. NKG2D-DAP10 triggers human NK cell-mediated killing via a Syk-independent regulatory pathway. *Nat Immunol* 2003;4:557–564. [PubMed: 12740575]
33. Tassi I, Le Friec G, Gilfillan S, Takai T, Yokoyama WM, Colonna M. DAP10 associates with Ly49 receptors but contributes minimally to their expression and function in vivo. *Eur J Immunol* 2009;39:1129–1135. [PubMed: 19247984]
34. Inui M, Kikuchi Y, Aoki N, Endo S, Maeda T, Sugahara-Tobinai A, Fujimura S, Nakamura A, Kumanogoh A, Colonna M, Takai T. Signal adaptor DAP10 associates with MDL-1 and triggers osteoclastogenesis in cooperation with DAP12. *Proc Natl Acad Sci USA* 2009;106:4816–4821. [PubMed: 19251634]
35. Sutherland KA, Rogers HL, Tosh D, Rogers MJ. RANKL increases the level of Mcl-1 in osteoclasts and reduces bisphosphonate-induced osteoclast apoptosis in vitro. *Arthritis Res Ther* 2009;11:R58. [PubMed: 19405951]
36. Cella M, Buonsanti C, Strader C, Kondo T, Salmaggi A, Colonna M. Impaired differentiation of osteoclasts in TREM-2-deficient individuals. *J Exp Med* 2003;198:645–651. [PubMed: 12913093]
37. Yogo K, Mizutamari M, Mishima K, Takenouchi H, Ishida-Kitagawa N, Sasaki T, Takeya T. Src homology 2 (SH2)-containing 5'-inositol phosphatase localizes to podosomes, and the SH2 domain is implicated in the attenuation of bone resorption in osteoclasts. *Endocrinology* 2006;147:3307–3317. [PubMed: 16601135]
38. Faccio R, Zou W, Colaianni G, Teitelbaum SL, Ross FP. High dose M-CSF partially rescues the Dap12^{-/-} osteoclast phenotype. *J Cell Biochem* 2003;90:871–883. [PubMed: 14624447]
39. Kaifu T, Nakahara J, Inui M, Mishima K, Momiyama T, Kaji M, Sugahara A, Koito H, Ujike-Asai A, Nakamura A, Kanazawa K, Tan-Takeuchi K, Iwasaki K, Yokoyama WM, Kudo A, Fujiwara M, Asou H, Takai T. Osteopetrosis and thalamic hypomyelination with synaptic degeneration in DAP12-deficient mice. *J Clin Invest* 2003;111:323–332. [PubMed: 12569157]
40. N'Diaye EN, Branda CS, Branda SS, Nevarez L, Colonna M, Lowell C, Hamerman JA, Seaman WE. TREM-2 (triggering receptor expressed on myeloid cells 2) is a phagocytic receptor for bacteria. *J Cell Biol* 2009;184:215–223. [PubMed: 19171755]
41. Hayashi A, Ohnishi H, Okazawa H, Nakazawa S, Ikeda H, Motegi S, Aoki N, Kimura S, Mikuni M, Matozaki T. Positive regulation of phagocytosis by SIRP β and its signaling mechanism in macrophages. *J Biol Chem* 2004;279:29450–29460. [PubMed: 15123631]
42. Fortin CF, Lesur O, Fulop T Jr. Effects of TREM-1 activation in human neutrophils: Activation of signaling pathways, recruitment into lipid rafts and association with TLR4. *Int Immunol* 2007;19:41–50. [PubMed: 17098818]
43. Bakker AB, Baker E, Sutherland GR, Phillips JH, Lanier LL. Myeloid DAP12-associating lectin (MDL)-1 is a cell surface receptor involved in the activation of myeloid cells. *Proc Natl Acad Sci USA* 1999;96:9792–9796. [PubMed: 10449773]

44. Beitz LO, Fruman DA, Kurosaki T, Cantley LC, Scharenberg AM. SYK is upstream of phosphoinositide 3-kinase in B cell receptor signaling. *J Biol Chem* 1999;274:32662–32666. [PubMed: 10551821]
45. Jiang K, Zhong B, Gilvary DL, Corliss BC, Vivier E, Hong-Geller E, Wei S, Djeu JY. Syk regulation of phosphoinositide 3-kinase-dependent NK cell function. *J Immunol* 2002;168:3155–3164. [PubMed: 11907067]
46. Arndt PG, Suzuki N, Avdi NJ, Malcolm KC, Worthen GS. Lipopolysaccharide-induced c-Jun NH2-terminal kinase activation in human neutrophils: Role of phosphatidylinositol 3-kinase and Syk-mediated pathways. *J Biol Chem* 2004;279:10883–10891. [PubMed: 14699155]
47. Honma M, Higuchi O, Shirakata M, Yasuda T, Shibuya H, Iemura S, Natsume T, Yamanashi Y. Dok-3 sequesters Grb2 and inhibits the Ras-Erk pathway downstream of protein-tyrosine kinases. *Genes Cells* 2006;11:143–151. [PubMed: 16436051]
48. Stork B, Neumann K, Goldbeck I, Alers S, Kähne T, Naumann M, Engelke M, Wienands J. Subcellular localization of Grb2 by the adaptor protein Dok-3 restricts the intensity of Ca²⁺ signaling in B cells. *EMBO J* 2007;26:1140–1149. [PubMed: 17290227]
49. Ng CH, Xu S, Lam KP. Dok-3 plays a nonredundant role in negative regulation of B-cell activation. *Blood* 2007;110:259–266. [PubMed: 17363732]
50. Hazen AL, Smith MJ, Despons C, Winter O, Moser K, Kerr WG. SHIP is required for a functional hematopoietic stem cell niche. *Blood* 2009;113:2924–2933. [PubMed: 19074735]
51. Tridandapani S, Phee H, Shivakumar L, Kelley TW, Coggeshall KM. Role of SHIP in FcγRIIb-mediated inhibition of Ras activation in B cells. *Mol Immunol* 1998;35:1135–1146. [PubMed: 10395202]
52. Tridandapani S, Pradhan M, LaDine JR, Garber S, Anderson CL, Coggeshall KM. Protein interactions of Src homology 2 (SH2) domain-containing inositol phosphatase (SHIP): Association with Shc displaces SHIP from FcγRIIb in B cells. *J Immunol* 1999;162:1408–1414. [PubMed: 9973396]

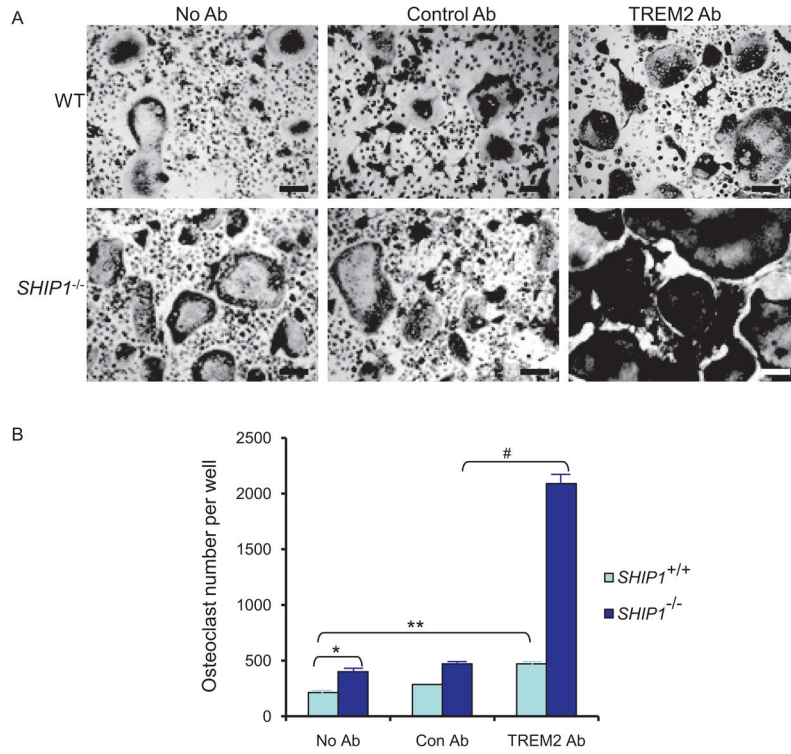


Fig. 1. SHIP1 inhibits enhanced osteoclastogenesis stimulated by the ligation of TREM2. Bone marrow-derived macrophage precursors were isolated from WT or *SHIP1*-deficient mice. Cells were treated with plate-bound antibody against TREM2 or control antibody together with RANKL (50 ng/ml) and M-CSF (20 ng/ml) for 5 days. The number of TRAP-positive osteoclasts that contained more than two nuclei were counted per well. **(A)** Osteoclast cultures were fixed and stained for TRAP. **(B)** Compared to cultures of WT cells, cultures of *SHIP1*-deficient cells formed twice as many osteoclasts ($*P < 0.01$). Ligation of TREM2 led to a twofold increase in the number of WT osteoclasts ($**P < 0.01$) and a fourfold increase in *SHIP1*-deficient osteoclasts ($^{\#}P < 0.002$). Data are representative of two experiments.

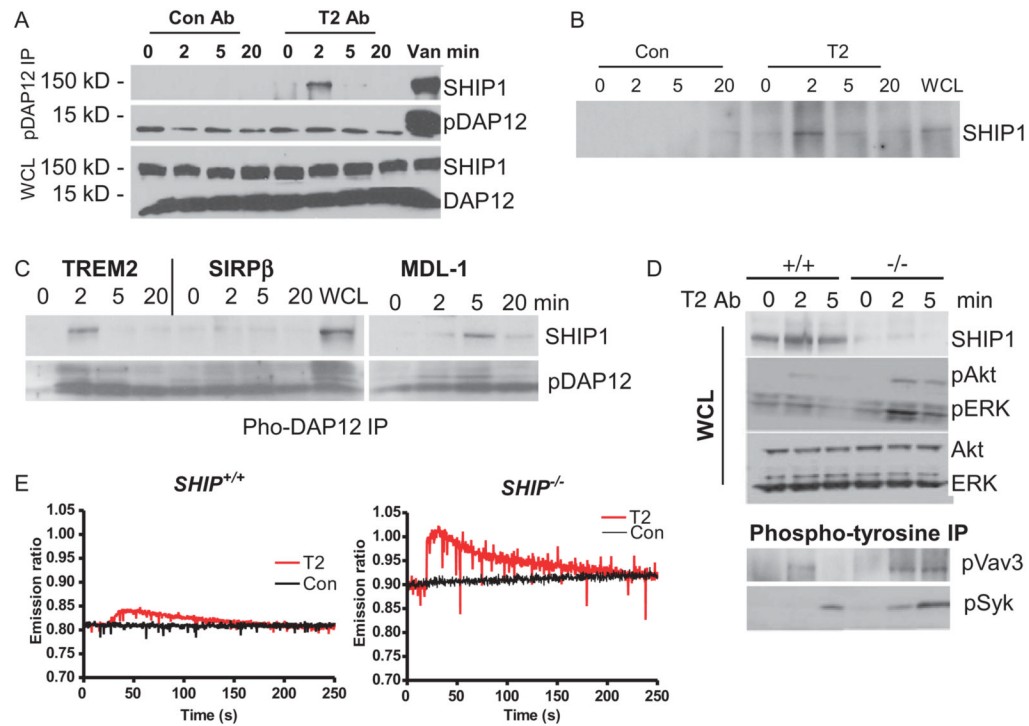


Fig. 2.

SHIP1 is recruited to DAP12 after ligation of TREM2 and it inhibits TREM2 and DAP12 signaling and Ca^{2+} flux. (A) Activation of TREM2 and DAP12 induces the association of SHIP1 with DAP12 in J774 cells stimulated with antibody against TREM2 (T2 Ab) but not in cells stimulated with control Ab (Con Ab). Samples from immunoprecipitations (IP) with antibody against pDAP12 were analyzed by Western blotting for the presence of SHIP1 and DAP12. Whole-cell lysates (WCL) were also analyzed similarly for the presence of SHIP1 and DAP12. Vanadate (Van) increased the amount of SHIP1 that coimmunoprecipitated with pDAP12. (B) BMMs stimulated with antibody against TREM2 or with control antibody were used in immunoprecipitation reactions with antibody against pDAP12 and were analyzed by Western blotting for the presence of SHIP1. (C) J774 cells were stimulated with antibodies against TREM2, SIRP β , or MDL-1 and then used in immunoprecipitation reactions with antibody against pDAP12. Stimulation with antibodies against TREM2 or MDL-1 induced the association of SHIP1 with DAP12, whereas stimulation with antibody against SIRP β did not. (D) BMMs derived from WT (+/+) or *SHIP1*-deficient (-/-) mice were treated by ligation of TREM2 and WCLs were analyzed by Western blotting for the presence of pAkt, pERK, and SHIP1. Membranes were stripped and incubated with antibodies against total ERK and Akt. Cell lysates were used in immunoprecipitation reactions with an antibody against phosphorylated tyrosine (pY) residues and analyzed by Western blotting for the presence of pVav3 and pSyk. (E) Ca^{2+} flux was induced in WT and *SHIP1*-deficient BMMs by antibody against TREM2 (red lines), whereas control antibody (black lines) had no effect. Ligation of TREM2 induced enhanced Ca^{2+} flux in *SHIP1*-deficient cells ($P = 0.0123$ for area under the curve). Data are representative of two studies for (B) and (C) and three studies for (A), (D), and (E).

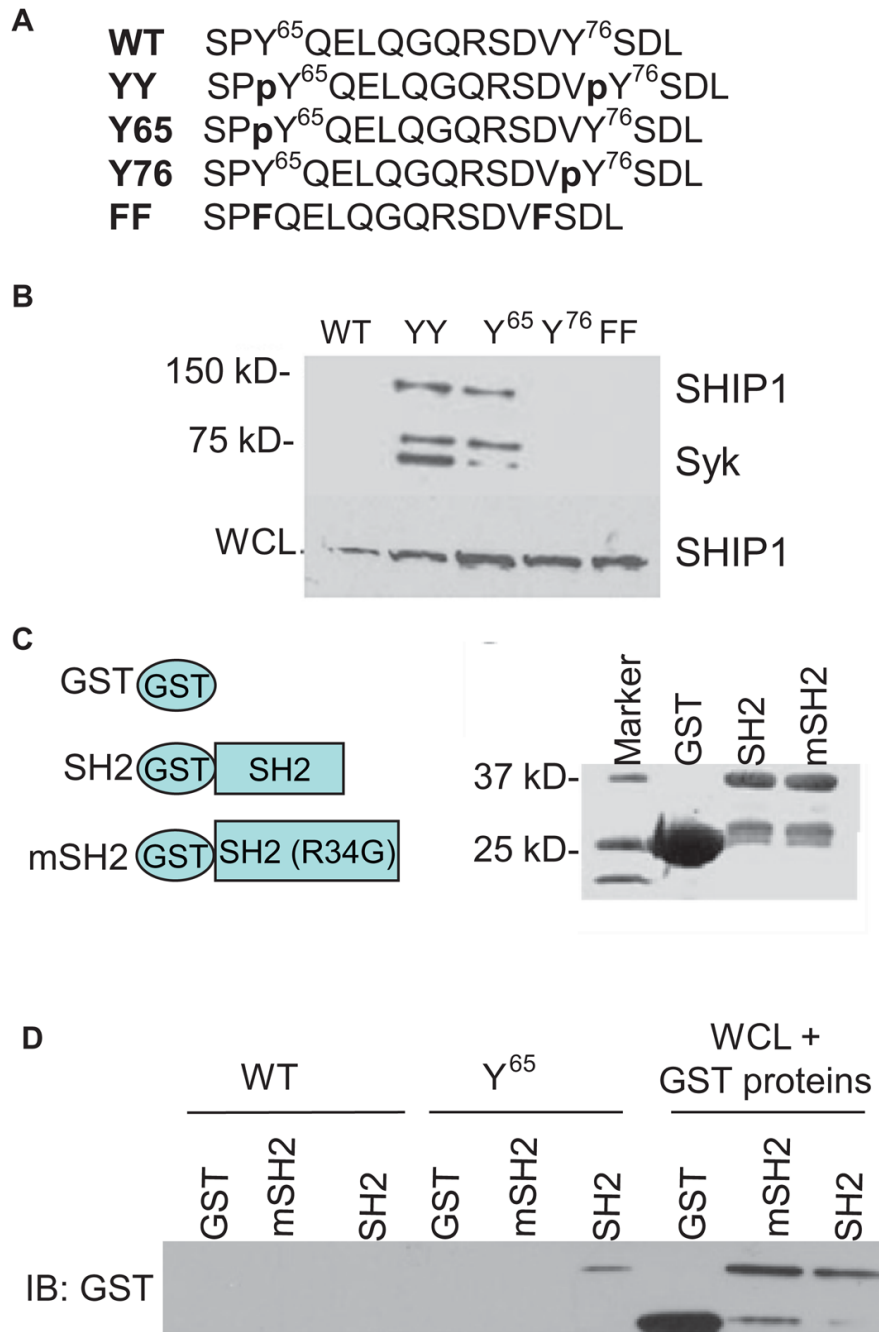


Fig. 3. SHIP1 binds directly to the phosphorylated ITAM in DAP12. **(A)** Biotinylated DAP12 ITAM peptides are listed. The specific phosphorylated tyrosine is noted by a lowercase p. Abbreviations for the amino acids are as follows: D, Asp; E, Glu; G, Gly; L, Leu; P, Pro; Q, Gln; R, Arg; S, Ser; V, Val; and Y, Tyr. **(B)** Lysates from resting RAW 264.7 cells were incubated with biotinylated peptides (10 μ M) overnight at 4°C. Peptide-protein complexes were precipitated with NeutrAvidin-conjugated beads and analyzed by Western blotting with antibodies against SHIP or Syk. WCLs were analyzed for the presence of SHIP1 as a loading control. **(C)** Schematic representation of the expression constructs that encode GST-SH2 fusion proteins of WT SHIP1 or an SH2 domain mutant of SHIP1 that contains a glycine in the place

of arginine at position 34 (R34G) (GST-mSH2). Coomassie blue staining of purified GST-fusion proteins is shown on the right. GST is ~25 kD, SH2 and mSH2 are ~37 kD. **(D)** The purified fusion proteins, GST, SH2, and mSH2 were incubated with biotinylated WT or phosphorylated Y⁶⁵ ITAM peptides overnight at 4°C, precipitated with NeutrAvidin beads, and analyzed by Western blotting with an antibody against GST. Purified GST-fusion proteins were incubated with antibody against GST to reveal the amount of fusion proteins added to the peptides. Data are representative of three studies.

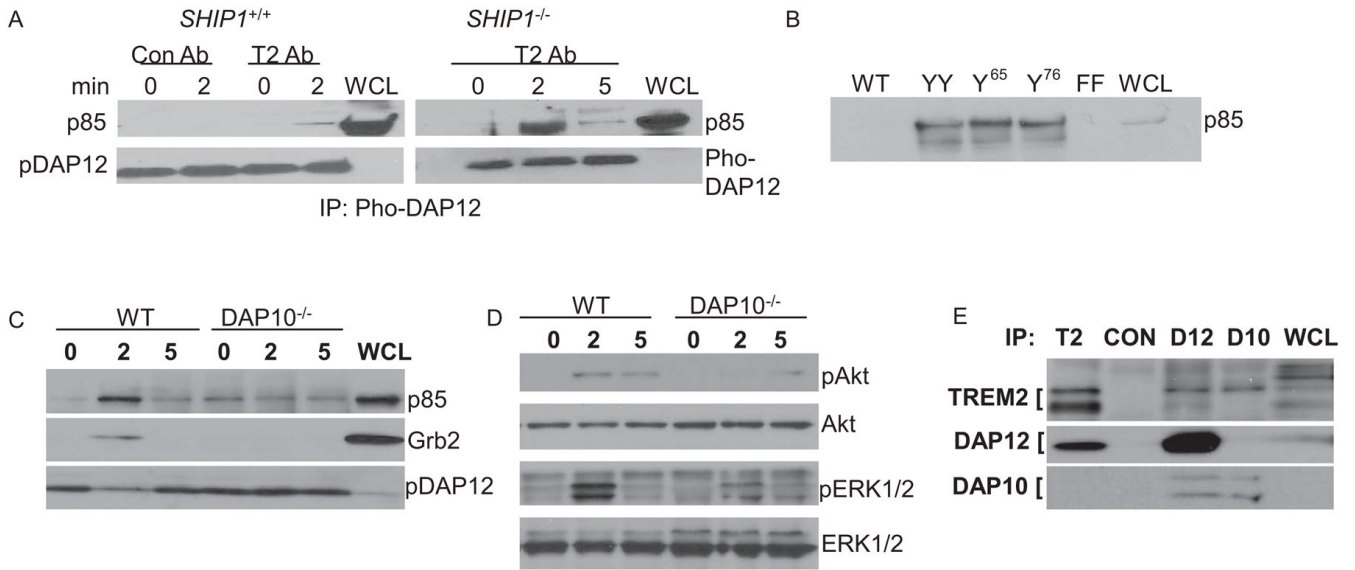


Fig. 4. DAP10-dependent recruitment of PI3K p85 mediates TREM2- and DAP12-dependent activation of Akt and ERK1/2. **(A)** WT (+/+) and *SHIP1*-deficient (-/-) BMMs were stimulated with antibody against TREM2 or with control antibody, lysed, subjected to immunoprecipitation with an antibody against pDAP12, and analyzed by Western blotting with antibodies against PI3K p85 or pDAP12. **(B)** Biotinylated DAP12 pITAM peptides coprecipitated with p85 in BMM lysates. **(C)** WT and *DAP10*-deficient BMMs were stimulated with antibody against TREM2. Samples subjected to immunoprecipitation with antibody against pDAP12 were analyzed by Western blotting for the presence of SHIP1, p85, and Grb2. **(D)** WCLs were analyzed by Western blotting with antibodies against pAkt, ERK1/2, and DAP12. Blots were stripped and incubated with antibodies against total Akt and ERK1/2. **(E)** WT macrophages were lysed in digitonin buffer and then subjected to immunoprecipitation reactions with antibodies against TREM2, DAP12, or DAP10 or with control antibody. Immunoprecipitated complexes were analyzed by Western blotting for each of these proteins. TREM2 was immunoprecipitated with DAP12 and DAP10. Data are representative of two experiments.

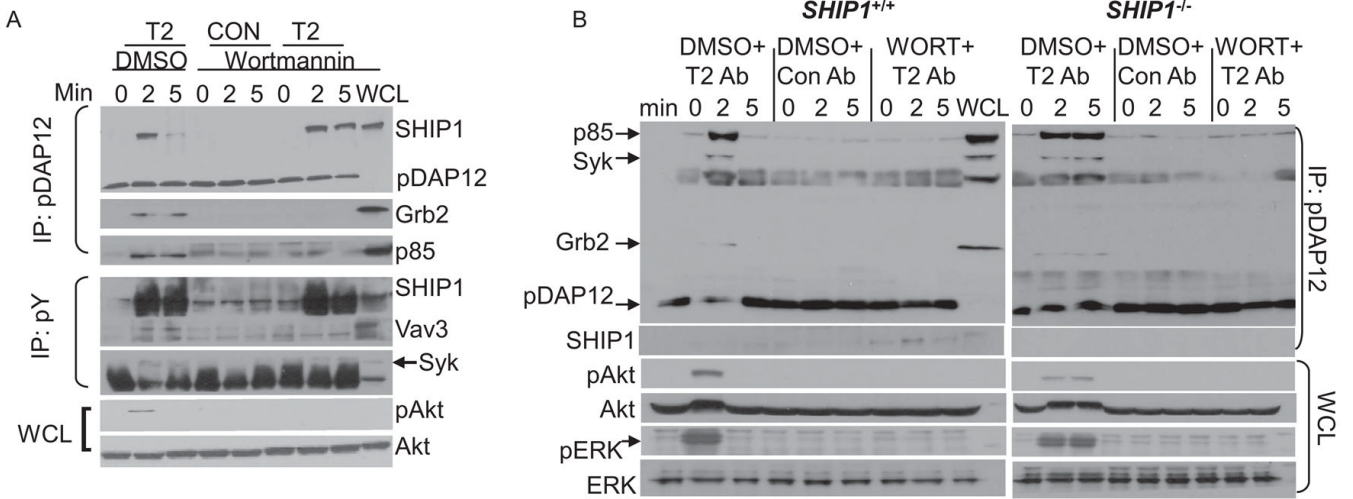


Fig. 5. Inhibition of PI3K activity enhances the recruitment of SHIP1 to DAP12 after ligation of TREM2. **(A)** J774 cells were treated with DMSO or wortmannin (0.2 μ M) before stimulation with antibody against TREM2 or with control antibody. Samples subjected to immunoprecipitation with antibody against pDAP12 were analyzed by Western blotting for the presence of SHIP1, Grb2, p85, and pDAP12. Lysates were subsequently subjected to immunoprecipitation with antibody against pY and analyzed by Western blotting for the presence of SHIP1, Vav3, and Syk. WCLs were analyzed by Western blotting for the presence of pAkt and total Akt. Data are representative of three experiments. **(B)** BMMs derived from WT or *SHIP1*-deficient mice were treated with wortmannin or DMSO and incubated with antibody against TREM2 or with control antibody. Lysates were subjected to immunoprecipitation with antibody against pDAP12 and analyzed by Western blotting for the presence of p85, Syk, Grb2, pDAP12, and SHIP1. WCLs were similarly analyzed for the presence of pAkt and pERK. Membranes were stripped and incubated with antibodies against total Akt or ERK. Data are representative of two experiments.

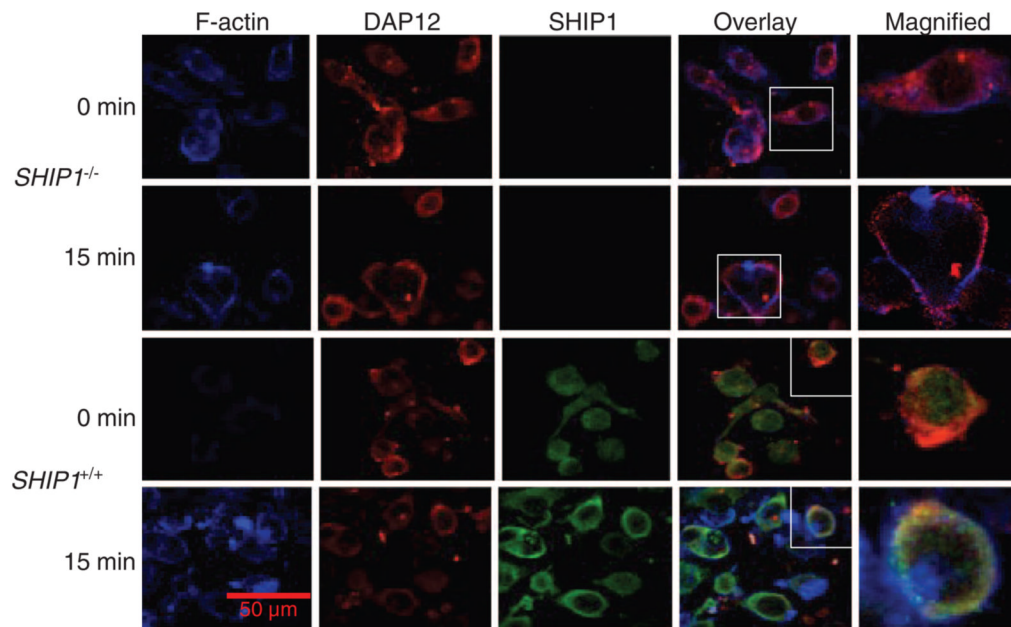


Fig. 6. Ligation of TREM2 induces the intracellular colocalization of SHIP1, F-actin, and DAP12 in osteoclasts. Osteoclasts derived from WT or *SHIP1*-deficient BMMs were prepared on eight-well paradox chamber slides, as described in Materials and Methods. Osteoclasts were starved of serum for 4 hours and treated with antibody against TREM2 for 15 min. Unstimulated (0 min) and stimulated cells were fixed and incubated with antibody against DAP12 (shown in red), phalloidin to detect F-actin (shown in blue), and antibody against SHIP1 (shown in green). The overlay shows the areas of colocalization of DAP12, F-actin, and SHIP1 at the plasma membrane. Data are representative of five studies.

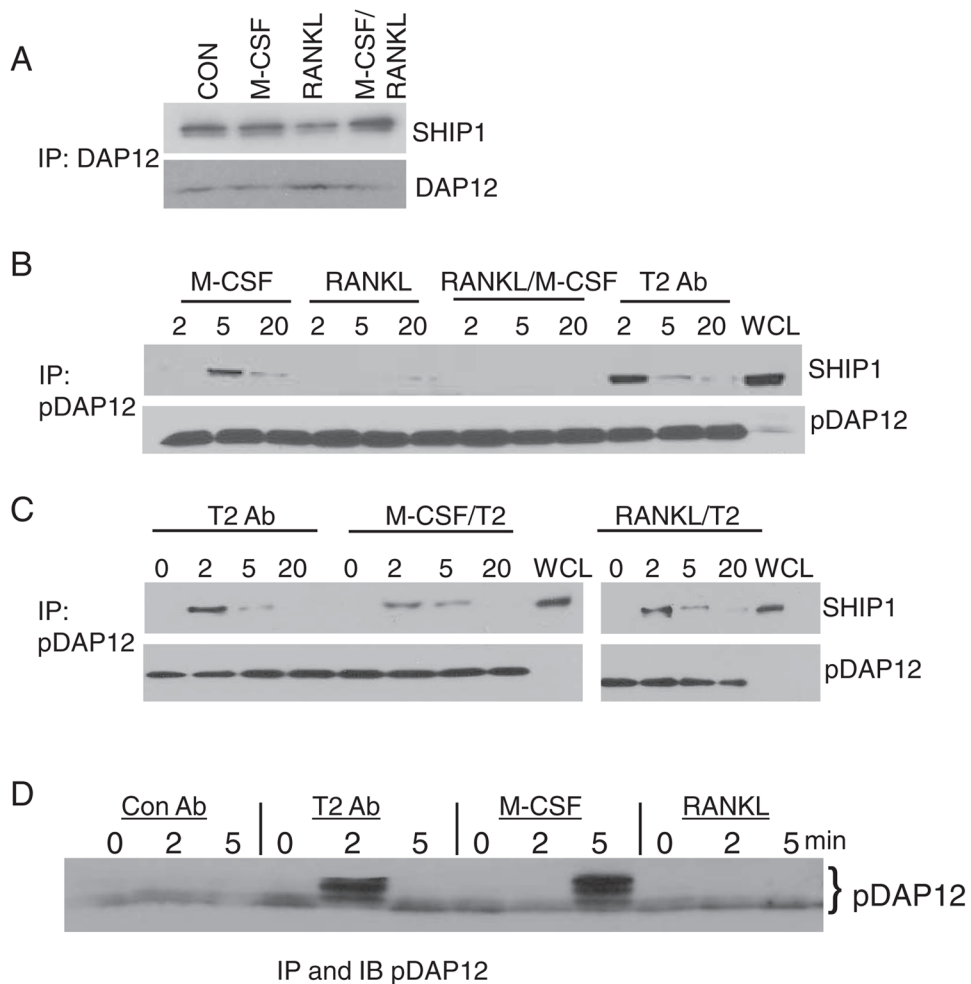


Fig. 7. Stimulation with RANKL and M-CSF leads to the recruitment of SHIP1 to DAP12. **(A)** RAW 264.7 cells were treated with control medium or with medium containing M-CSF (20 ng/ml), RANKL (50 ng/ml), or both for 3 days. Adherent cells were lysed on the plates and subjected to immunoprecipitation with antibody against DAP12. Complexes were analyzed by Western blotting for the presence of SHIP1 and DAP12. **(B)** J774 cells in suspension were treated with RANKL (100 ng/ml), M-CSF (100 ng/ml), or both or were treated with antibody against TREM2 for up to 20 min. Samples subjected to immunoprecipitation with antibody against pDAP12 were analyzed by Western blotting for the presence of SHIP1 and pDAP12. **(C)** J774 cells were stimulated in suspension with antibody against TREM2 alone, or in the presence of RANKL or M-CSF. Cells were subjected to immunoprecipitation with antibody against pDAP12 and immunoprecipitates were analyzed by Western blotting with antibodies against SHIP1 or pDAP12. **(D)** A different antibody against pDAP12 (2426) was used to immunoprecipitate pDAP12 from RAW 264.7 cells and the resulting immunoprecipitates were analyzed by Western blotting for pDAP12. Data are representative of three experiments.

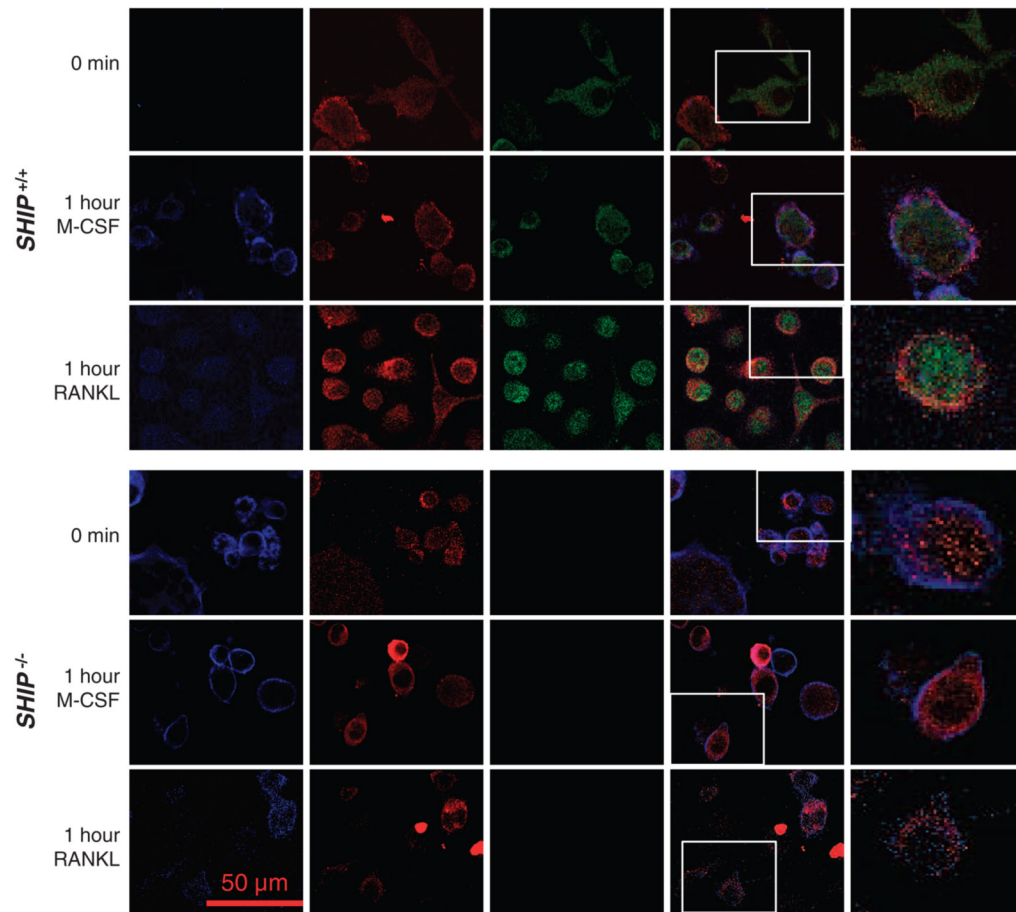


Fig. 8. M-CSF and RANKL differentially induce the colocalization of SHIP1 and DAP12. WT and *SHIP1*-deficient BMMs were differentiated to osteoclasts by culturing with M-CSF and RANKL for 3 days. After being starved of serum for 4 hours, cells were treated with M-CSF (100 ng/ml) or RANKL (100 ng/ml) for 4 hours, fixed, and incubated with antibody against DAP12 (shown in red), phalloidin (shown in blue), or antibody against SHIP1 (shown in green).

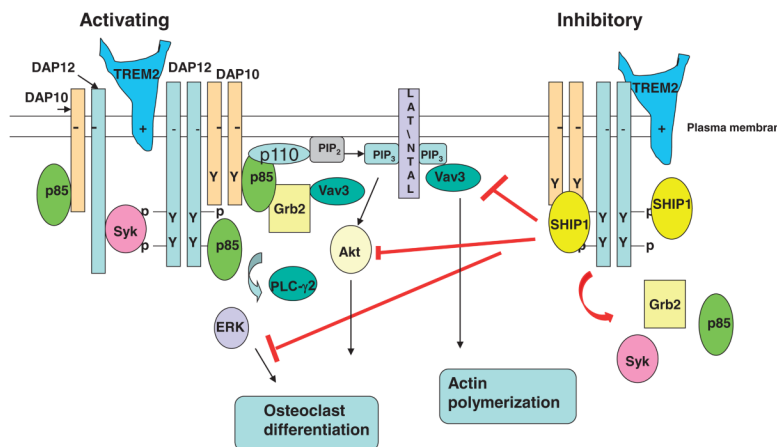


Fig. 9. Proposed DAP12 signaling pathway in macrophages and osteoclasts. In response to ligation of TREM2, Src family kinases phosphorylate the ITAM of DAP12 and the YINM motif of DAP10, which form docking sites for the Syk and p85, with the subsequent recruitment of PLC-γ2 and Grb2. This signaling complex then leads to the activation of Akt, ERK1/2, and Vav3. Simultaneously, SHIP1 is recruited to the DAP12 ITAM where it may dislodge or prevent the further recruitment of SH2 domain-containing proteins, including p85 and Syk. This leads to an arrest in the activation of PI3K, ERK, Akt, and VAV3. The absence of SHIP1 enables prolonged signaling in response to the activation of DAP12, which leads to enhanced osteoclastogenesis. Low-avidity ligands of macrophages or bacteria may preferentially recruit SHIP1, whereas high-avidity ligands or receptor cross-linking may induce a strong activation of PI3K and Syk.